

## Chapter 8

# Timing, Distribution, and Volume of Proximal Products of the 2006 Eruption of Augustine Volcano

By Michelle L. Coombs<sup>1</sup>, Katharine F. Bull<sup>2</sup>, James W. Vallance<sup>3</sup>, David J. Schneider<sup>1</sup>, Evan E. Thoms<sup>1</sup>, Rick L. Wessels<sup>1</sup>, and Robert G. McGimsey<sup>1</sup>

### Abstract

During and after the 2006 eruption of Augustine Volcano, we compiled a geologic map and chronology of new lava and flowage deposits using observational flights, oblique and aerial photography, infrared imaging, satellite data, and field investigations. After approximately 6 months of precursory activity, the explosive phase of the eruption commenced with two explosions on January 11, 2006 (events 1 and 2) that produced snow-rich avalanches; little or no juvenile magma was erupted. Seismicity suggests that a small lava dome may have extruded on January 12, but, if so, it was subsequently destroyed. A series of six explosions on January 13–14 (events 3–8) produced widespread but thin (0–30 cm) pyroclastic-current deposits on the upper flanks above 300 m altitude and lobate, 0.5- to 2-m-thick pyroclastic flows that traveled down most flanks of the volcano. Between January 14 and 17, a smooth lava lobe formed in the east half of the roughly 400-m-wide summit crater and was only partially covered by later deposits. An explosion on January 17 (event 9) opened a crater in the new lava dome and produced a ballistic fall deposit and pyroclastic flow on the southwest flank. During the interval from January 17 to 27, a rubbly lava dome effused. On January 27, explosive event 10 generated a pyroclastic current that left a deposit, rich in dense clasts, on the north-northwest flank. Immediately following the pyroclastic current, a voluminous 4.7-km-long pyroclastic flow swept down the north flank. Three more explosive blasts on January 27 and 28 produced unknown but likely minor on-island deposits. The cumulative

volume of erupted material from the explosive phase, including domes, flows, and fall deposits (Wallace and others, this volume), was  $30 \times 10^6$  m<sup>3</sup> dense-rock equivalent (DRE).

The continuous phase of the eruption (January 28 through February 10) began with a 4-day period of nearly continuous block-and-ash flows, which deposited small individual flow lobes that cumulatively formed fans to the north and northeast of the summit. A single larger pyroclastic flow on January 30 formed a braided deposit on the northwest flank. Roughly  $9 \times 10^6$  m<sup>3</sup> (DRE) of magma erupted during this period. Around February 2, the magma flux rate waned and a northward lava flow effused and reached a length of approximately 900 m by February 10. Approximately  $11 \times 10^6$  m<sup>3</sup> (DRE) of magma erupted during the second half of the continuous phase.

After a 23-day hiatus, lava effusion recommenced in early March (the effusive phase) and was accompanied by frequent (but volumetrically minor) block-and-ash flows. From March 7 to 14, extrusion increased markedly; two blocky lava-flow lobes, each tens of meters thick, moved down the north and northeast flank of the volcano; and a new summit lava dome grew to be ~70 m taller than the pre-2006 summit. This phase produced  $26 \times 10^6$  m<sup>3</sup> (DRE) of lava. Active effusion had ceased about March 16, but, in April and May, three gravitational collapses from the west margin of the north lava flow produced additional block-and-ash flows. The basic sequence of the 2006 eruption closely matches that of eruptions in 1976 and 1986.

### Introduction

The 2006 eruption of Augustine Volcano was monitored at an unprecedented level of detail for an Alaskan volcano. Precursory activity was detected by a network of seismic and GPS instruments, airborne gas measurements, and thermal and satellite data. As the eruption commenced in January of 2006, these tools were augmented by on-island remote cameras, helicopter-based thermal imaging, pressure sensors, and more. Despite the

---

<sup>1</sup>Alaska Volcano Observatory, U.S. Geological Survey, 4200 University Drive, Anchorage, AK 99508.

<sup>2</sup>Alaska Volcano Observatory, Alaska Division of Geological and Geophysical Surveys, 3354 College Road, Fairbanks, AK 99709.

<sup>3</sup>U.S. Geological Survey, Cascades Volcano Observatory, 1300 SE Cardinal Court, Vancouver, WA 98683.

volcano's remote location on Augustine Island, 115 km from Homer, Alaska, the Alaska Volcano Observatory (AVO) was able to follow closely the course of the eruption and correlate visual and thermal changes, geophysical signals, and eruptive deposits to gain a better understanding of the eruptive processes at work at this most active of Cook Inlet volcanoes.

The 2006 eruption unfolded in a series of three distinct phases (Power and others, 2006): an explosive phase of 17 days duration (January 11 to 28); a continuous phase of 13 days duration (January 28 to February 10); and an effusive phase of 13 days duration (March 3 to 16). The phases were distinguished by variations in eruptive style and magma composition (Larsen and others, this volume; Power and Lalla, this volume; Vallance and others, this volume; Wallace and others, this volume) and by corresponding deformation of the edifice (Cervelli and others, this volume). The overall sequence was similar to other historical eruptions of Augustine Volcano: beginning with an explosive onset, followed by lessening intensity, and finally concluding with an effusive phase (Power and others, 2006).

In this paper, we present a detailed chronology of the geologic events during the 2006 eruption, describing how and when on-island deposits (lava flows and domes and pyroclastic-flow, lahar, and avalanche deposits) were produced. The 2006 sequence was mostly determined as the eruption progressed, primarily from seismicity and numerous observational overflights, combined with aerial photographs, remotely operated on-island cameras, and satellite imagery. Continued analysis of the data generated during the eruption, as well as study of the stratigraphy of erupted deposits, has allowed us to further refine the timeline of events and their resulting deposits, sometimes deposit by deposit.

In addition to the chronology, we present a geologic map of the on-island deposits from the 2006 eruption (plate 1). The map was initially generated during the eruption but was greatly refined during a field campaign in the summer of 2006. Initiating the mapping as the eruption progressed allowed us to map the new deposits in a level of spatial and temporal detail not previously possible for the eruption of an Alaskan volcano. In some cases, we are able to distinguish deposits erupted during individual, minutes-long explosive events. Map units are introduced in the text in the order in which they were emplaced, and the Description of Map Units is found on the accompanying plate. Vallance and others (this volume) and Larsen and others (this volume) provide descriptions of the sedimentology and petrology, respectively, of the erupted products. The 2006 deposit map depicts sometimes ephemeral deposits and is meant to augment the more comprehensive geologic map of the island (Waite and Béget, 2009).

Finally, we present volume estimates for individual deposits and combine these with our temporal framework to infer the time-eruptive volume progression of the eruption. In addition, component studies of the deposits reveal shifts in the composition of magmas feeding the eruption (Vallance and others, this volume) and, by combining component and volume data, we quantify the fluxes of two magmatic compositional end

members. We show that the explosive phase produced pyroclastic flows initially rich in a low-silica andesite (57 weight percent  $\text{SiO}_2$ ) that become progressively more silica rich and voluminous. The continuous-phase deposits, rich in high-silica andesite (62.5 weight percent  $\text{SiO}_2$ ), are consistent with nearly continual spalling, degradation, and collapse of a rapidly growing summit lava dome. The effusive phase marked a change back to the low-silica andesite. These observations provide a framework within which we evaluate underlying magmatic processes that drove the eruption and show how eruptive style relates to magma flux.

## Geologic Background

Augustine Volcano is an island volcano, located in upper Cook Inlet in south-central Alaska, that is part of the eastern Aleutian volcanic arc. Located 275 km southwest of Anchorage and 115 km west-southwest of Homer, Augustine Island is roughly circular, 9 km by 11 km in diameter, and Augustine Volcano reached an altitude of 1,260 m prior to the 2006 eruption. The volcano comprises a summit dome complex surrounded by an apron of pyroclastic and debris-avalanche deposits. On the south shoulder of the volcano, sedimentary rocks of the Jurassic Naknek Formation crop out from sea level to 400 m above sea level (asl) (Waite and Béget, 2009).

The oldest known products of Augustine Volcano are late Pleistocene in age and comprise bedded hyaloclastite of olivine basalt and dense juvenile rhyolite (Johnston, 1978). Records of early to middle Holocene Augustine eruptions are scarce and limited to a few small tephra exposures on the south flank and some distal ashes with Augustine compositional affinities (Waite and Béget, 2009). The late Holocene, prehistoric eruptive record is more complete and shows that Augustine often erupted explosively, producing sometimes thick tephra falls, an apron of flowage deposits, and an edifice consisting of overlapping lava domes and short lava flows (Waite and Béget, 2009). In addition, the late Holocene has been marked by repeated edifice failures and debris avalanches, as recent as 1883 (Béget and Kienle, 1992). Augustine has erupted historically in 1883, 1935, 1964, 1976, and 1986, each time producing andesitic through dacitic fall deposits, pyroclastic flows, and lava domes.

The last several eruptions of Augustine Volcano have been remarkably similar in eruptive style and compositions of erupted material, and the 2006 eruption was no exception. In particular, the 2006 eruption followed a pattern similar to the 1976 eruption. After roughly 9 months of precursory seismicity, the 1976 eruption commenced on January 22 with 3 days of 13 explosive events, the first of which excavated a large crater at the summit that was 550 m by 350 m across and 200 m deep (Johnston, 1979; Swanson and Kienle, 1988; Power and Lalla, this volume). After a quiescent period of 12 days, the volcano then entered another, slightly less explosive phase from February 6 through 15, when it produced northward-directed, lithic-rich pyroclastic flows and, during the second half of this

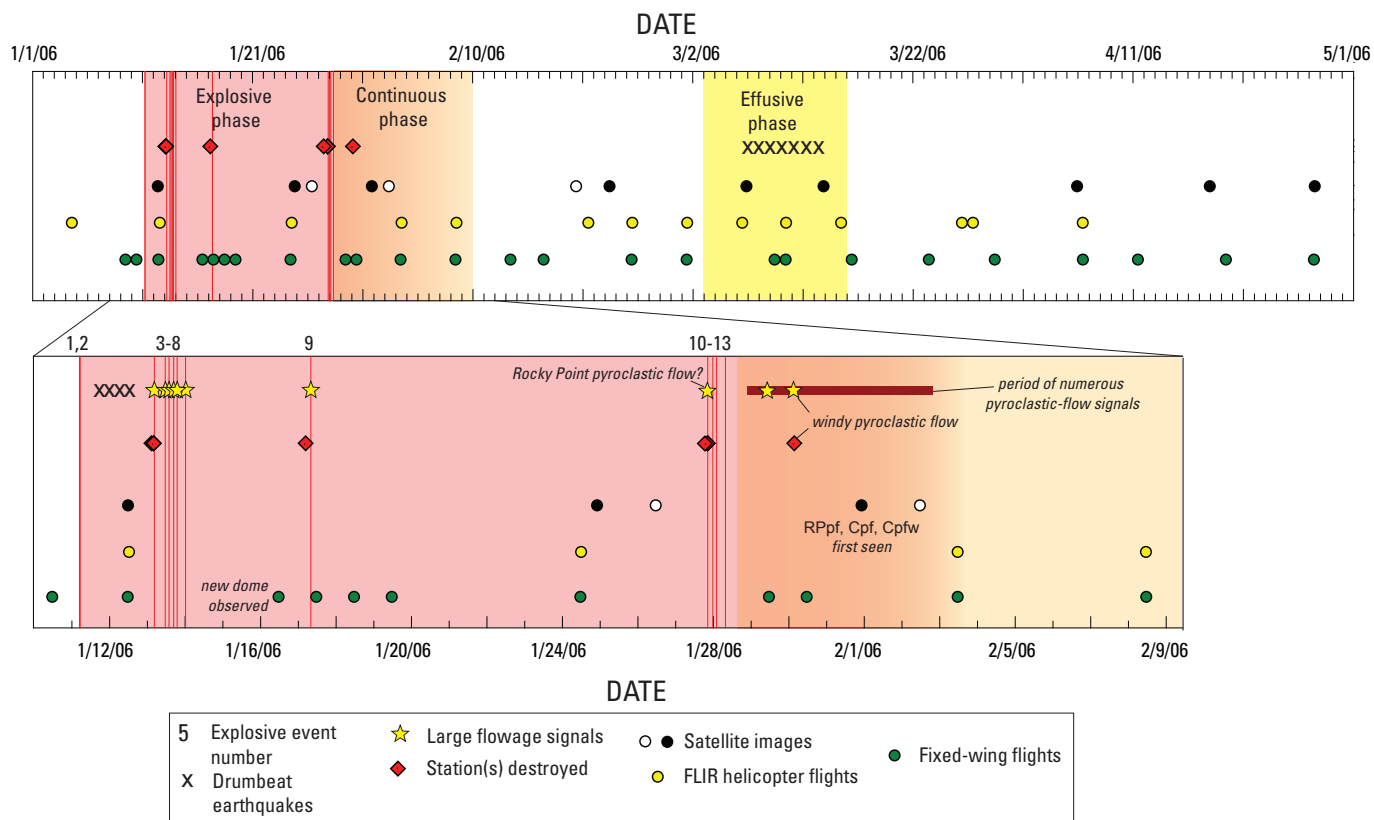


**Figure 1.** Timeline of eruptive events and observations during the 2006 eruption. Vertical red lines indicate timing of explosive-phase events 1–13. Timing of drumbeat earthquakes from Power and Lalla (this volume). For satellite images, open circles are Hyperion data, black circles are ASTER data (see Wessels and others, this volume, for details). Colored fields indicate the three eruptive phases defined in the text; transition from dark to light orange within continuous phase marks transition from pyroclastic-flow to lava-flow activity.

interval, a summit lava dome (Stith and others, 1977; Kamata and others, 1991). This phase resembled the 2006 continuous phase in the duration, progression, and character of the resulting deposits. After tapering effusive activity through February 1976, the final stage of the eruption occurred April 13 through 18 with expansion of the lava dome and shedding of accompanying block-and-ash flows (Johnston, 1978). The Kamata and others (1991, figs. 2, 3) map of the 1976 deposits mimics the distribution of the 2006 deposits.

The 1986 eruption sequence resembles the 1976 and 2006 sequences but with some distinct differences. The 1986 eruption also began with approximately 9 months of precursory, shallow seismicity, followed by a 12-day-long explosive phase marked by a series of discrete explosions (Power, 1988). After a 13-day lull, the first dome-building phase began and was marked by the effusion of a lava dome and short, steep northward lava flow and numerous small pyroclastic flows (Yount and others, 1987; Power, 1988). This period was followed by 3 months of quiet and then a final dome-building phase in August of 1986. This final phase was accompanied by the growth of a lava spine atop the new dome and emplacement of multiple pyroclastic flows.

## Methods

Because of eruptive activity, field work on Augustine Island was limited throughout January and February 2006. Preliminary deposit maps were made using vertical and oblique aerial photos taken during observation flights, satellite imagery, and images acquired by remote on-island cameras (table 1; fig. 1). Because much of the eruption occurred in the winter, some deposits became covered by snow and were obscured in all images except those acquired immediately after emplacement. Those syn- and post-event images greatly aided the mapping process.

Photographs were taken with numerous digital cameras during field work, and observational and gas-measurement flights to and around Augustine Island that took place during the 2006 eruption. New deposits were often first observed and documented during such flights. At times, when vertical imagery was not also available, deposits would be roughly mapped using these oblique photos, and the exact locations would be refined when georeferenced imagery (orthophotos, for example) became available.

**Table 1.** List of observations and data used to compile deposit chronology.

[Main events shown in bold. For a complete list of flights, see Neal and others (this volume). For a complete list of satellite data and FLIR observations, see Wessels and others (this volume). For a complete list of low-light camera observations, see Sentman and others (this volume). Overflights and field work typically spanned over an hour or more and occurred around midday. Unit abbreviations are included in Observation column; for complete unit descriptions see plate 1]

<b>Date</b>	<b>Time (AKST unless noted)</b>	<b>Image type or eruptive event</b>	<b>Observation</b>	<b>Comments</b>
12/2/05		Overflight photographs		
12/12/05		Overflight photographs	Ash on surface; no flowage deposits	
12/20/05	12:37:00	ASTER daytime visual and thermal images	Two northeast-striking 250°C thermal features at summit	Thin clouds, but can see island
12/20/05		Overflight and fieldwork photographs	Snow-covered summit; ash seen on 12/12/2005 photos still visible below snow line; no flowage deposits	
12/22/05		Overflight and fieldwork photographs, FLIR	Snow-covered summit and flanks; no flowage deposits; some increased heat flow and fumarolic activity at summit with maximum temp. of at least 210°C	
1/4/06		Airphotos and orthophoto	Snow-covered flanks; no flowage deposits	
1/4/06		Overflight and fieldwork photos, FLIR	Snow-covered flanks; no flowage deposits; maximum summit fumarole temperature at least 390°C; overall heating of summit region	
1/10/06		Overflight photographs	Confirm that no flowage events are present	
<b>1/11/06</b>	<b>0444</b>	<b>Explosive event 1; beginning of explosive phase</b>		
<b>1/11/06</b>	<b>0512</b>	<b>Explosive event 2</b>		
1/11/06		Overflight photographs	First appearance of Exma on upper flanks	Lower flanks obscured by clouds
1/12/06	12:42:44	ASTER daytime VIS and thermal	Plume moving south	Mostly cloudy
1/12/06		Overflight and fieldwork photos, FLIR	Full extent of Exma from events 1 and 2 visible; ash from events 1 and 2 on north flank; low-level fluctuating ash emissions ongoing throughout day; new vent visible through 1986 dome, just south of 1986 spine	Better visibility than 1/11/2006
1/12/06		Burr Point camera photographs	Good views of north flank Exma	
<b>1/13/06</b>	<b>0424</b>	<b>Explosive event 3</b>		
<b>1/13/06</b>	<b>0847</b>	<b>Explosive event 4</b>		
1/13/06	0900	Burr Point camera photographs	Pyroclastic-flow-generated ash cloud on northeast and east flank; no active flows to north or northwest	Still rather dark. Cloud related to event 4
1/13/06	0915	Burr Point camera photographs	Coignimbrite cloud still present above northeast and east flanks; steaming, dark flow deposits are visible down north and northwest flanks	Significantly lighter than previous photo; flow deposits likely from event 3
1/13/06	0930 to 1115	Burr Point camera photographs	Ash cloud dissipates; steam rising from east flank is visible and it looks like most of the flows from event 4 flowed east	
1/13/06	0946	Mound camera photographs	Ash cloud mostly fills field of view; some sky visible in upper right (to the north)	
1/13/06	1032, 1039, 1106	Mound camera photographs	Ash plume rising straight up from vent; steam/ash rises from east flanks; some point-source steaming visible from surface of new flow(s)	
<b>1/13/06</b>	<b>1122</b>	<b>Explosive event 5</b>		

**Table 1.** List of observations and data used to compile deposit chronology.—Continued

Date	Time (AKST unless noted)	Image type or eruptive event	Observation	Comments
1/13/06	1130	Burr Point camera photographs	Plentiful ash billowing up from east flank, but also some ash/steam in foreground of photo on lower north flank; small Expf flow is seen making its way down the upper northwest flank	Five minutes after the end of event 5
1/13/06	1135	Mound camera photographs	Bushes visible in foreground, but rest of view is dark with gray airborne ash	
1/13/06	1145	Burr Point camera photographs	Dark ash cloud rising from summit and east flank; north flank has cleared and new dark Expf flows visible on upper north flank—one is still steaming, being emplaced? Newly steaming deposits low on north-northwest flank (lower right of photo)	
1/13/06	1206	Mound camera photographs	Ash rising from middle ground of image, plume above	
1/13/06	1428	Mound camera photographs	Nice views of new steaming flow deposits	
1/13/06	1630	Burr Point camera photographs	Plume, white in the last few images, appears to have become more ash rich and vigorous	
1/13/06	1638, 1640	Mound camera photographs	Image is darker, plume looks more ash rich	
<b>1/13/06</b>	<b>1640</b>	<b>Explosive event 6</b>		
1/13/06	1640 to 1714	Mound camera photographs	Series of dark images shows pyroclastic flow or surge coming toward camera	
1/13/06	1645	Burr Point camera photographs	Dark, billowing cloud rises from summit and east flank and covers east half of image; discrete pyroclastic flow descends just east of north lava flow; no flows on northwest flank	
1/13/06	1700 to 1715	Burr Point camera photographs	Ash from event 6 dissipates relatively quickly, only small plume from summit remains by 5:15	
<b>1/13/06</b>	<b>1858</b>	<b>Explosive event 7</b>		
1/13/06	unknown	Numerous satellite data sources	New vent visible in location of 1986 dome	
<b>1/14/06</b>	<b>0014</b>	<b>Explosive event 8</b>		
1/16/06		Overflight photographs	Summit has fresh snow; new lava dome visible (Exd1); many flank photos	Ash-covered unvegetated areas look deceptively like new flows
1/16/06	daytime	Mound camera photographs	New east flows visible underneath summit cloudcap	Camera view is now tilted
1/16/06		Numerous satellite data sources	Dome (Exd1) dimensions of 200 m by 160 m	
<b>1/17/06</b>	<b>0758</b>	<b>Explosive event 9</b>		
1/18/06		Overflight photographs	Entire island ash covered; ballistic blocks visible on upper south flank	Good lighting
1/21/06		Numerous satellite data sources	January 16 lava dome (Exd1) elongated; crater visible	
1/24/06		Aeromap airphotos	Good views of new Expf and Expct deposits on flank	Summit obscured by clouds
1/24/06		Overflight and fieldwork photographs, FLIR	Fresh snow on summit and flanks; light ash on southeast flank; dark, hot, steaming, levied flows on east, northeast, and north flanks; Exd1 visible on east part of summit, maximum temp of 140°C	Summit partially obscured by clouds/steaming
1/24/06	22:44:16	ASTER nighttime thermal	Thermal features at summit; weaker thermal features on flanks	Clear

**Table 1.** List of observations and data used to compile deposit chronology.—Continued

Date	Time (AKST unless noted)	Image type or eruptive event	Observation	Comments
1/26/06	12:03:15	Hyperion and ALI	Hot flowage deposits on northeast flank	Clear
<b>1/27/06</b>	<b>2024</b>	<b>Explosive event 10</b>		
<b>1/27/06</b>	<b>2337</b>	<b>Explosive event 11</b>		
<b>1/28/06</b>	<b>0204</b>	<b>Explosive event 12</b>		
<b>1/28/06</b>	<b>0742</b>	<b>Explosive event 13</b>		
1/28/06	1420	Mound camera photographs	Dark, billowing, ash-rich plume with white steam collar around its base above vent	
1/28/06	1429	Mound camera photographs	Plume looks slightly more energetic; ash raining to the south-southwest	
<b>1/28/06</b>	<b>1431</b>	<b>Explosive event 14; beginning of continuous phase</b>		
1/28/06	1418	Mound camera photographs	First sight of dark-gray ash in plume	
1/28/06	1431	Mound camera photographs	More ash falling; plume has bifurcated with second smaller arm rising more straight up; no flows are visible	
1/28/06	1436 to 1707	Mound camera photographs	Dark-gray plume present all afternoon until darkness falls; ash appears to rain to the south in all images	
1/29/06	1007 to 1015	Mound camera photographs	Thick billowing plume rises from summit and moves south; another ash cloud rises from north half of summit and moves down north flank	
1/29/06	1117	Strong (unnumbered) event		
1/29/06	1127	Homer camera photographs	Tall, wide plume visible above low clouds at top of image	
1/29/06	~1230	Overflight photographs	Island is ash covered and flows are steaming on west and north flanks	Photos from afar
1/29/06	1547 to 1642	Mound camera photographs	Images are starting to clear after being dark for most of the day; dark cloud seen moving south; blue sky in upper right (north); later in sequence cloud rises from north flank, then darkness sets in	
<b>1/30/06</b>	<b>0621</b>	<b>Strong (unnumbered) event</b>		
1/30/06		Overflight photographs	Views of plume from afar	No good island shots
1/30/06		Numerous satellite data sources	Two new lava lobes visible at summit (Exd2)	
1/31/06	22:50:44	ASTER nighttime thermal	RPpf and Cpfw visible; surface to east of RPpf obscured by plume	
2/2/06	11:53:18	Hyperion and ALI	Strong thermal features from dome at summit and block-and-ash flow down northeast flank	
2/3/06		Overflight and fieldwork photographs	White plume to 1,800 m asl; ash-rich plume rising from north flank	Volcano shrouded in clouds
<b>2/3/06</b>	<b>roughly 1200</b>	<b>Continuous-phase activity lessens</b>		
2/7/06		Numerous satellite data sources	900-m-long lava flow to north	
2/7/08	Night	Low-light camera in Homer	North flank pyroclastic-flow and lava activity	
2/8/06	0800 to 0830	Views from Homer	With binoculars, incandescent flows visible on north flank	

**Table 1.** List of observations and data used to compile deposit chronology.—Continued

Date	Time (AKST unless noted)	Image type or eruptive event	Observation	Comments
2/8/06	Morning	Mound camera photographs	Steaming (new dome?) at summit; grey (coignimbrite?) cloud on north flank	
2/8/06	midday	Overflight and fieldwork photographs, FLIR	Dark Cpf and RPpf flows on north flank in high contrast to fresh white snow; deposits range from 10 to 25°C with some bigger, hotter blocks	Summit obscured by lenticular cloud; first rock samples collected (from RPpf)
<b>2/10/06</b>		<b>Continuous phase ends; hiatus begins</b>		
2/16/06		Overflight photographs		Most of flanks obscured, but great summit views including dome
2/19/06	11:52:42	Hyperion satellite image	Smaller thermal feature at summit as compared to 2/2/06 image	
2/20/06		Overflight and fieldwork photographs; FLIR	Good views of Cpf, RPpf; visited deposits; Eff dome and north flow visible especially in FLIR images	Rock samples collected from Exlh, Expf, Cpf; summit obscured somewhat by steaming and clouds
2/21/06		Airphotos and orthophoto	Good coverage of north-flank flow deposits	Summit is obscured by steam
2/22/06	12:37:03	ASTER daytime visual and thermal	Good views of flows	
2/24/06		Numerous satellite data sources	1,000-m-long lava flow to north	
2/24/06		Overflight and fieldwork photographs; FLIR	Excellent views of summit, including north lava flow	
3/1/06		Overflight and fieldwork photographs	No apparent changes since 2/24/06	
<b>3/3/06</b>		<b>Effusive phase begins</b>		
3/4/06		Mound camera photographs	Ash emissions	
3/5/06	nighttime	Low-light camera in Homer	Incandescence traveling down northeast slope	Probably associated with avalanching from lava dome
3/6/06	0517 to 0702	Burr Point camera photographs	Incandescence near the summit; no flows travel down flanks	
3/6/06	0621	Low-light camera in Homer	Incandescence traveling down northeast slope	
3/6/06		Fieldwork photographs	Active pyroclastic flow down northeast chute; north lava flow visible; northeast lava flow has not yet formed	Clear weather; excellent views
3/6/06	1417	Mound camera photograph	Pyroclastic flow moving down north flank	Coincident with 3-minute-long seismic signal
3/6/06	1616	Burr Point camera photographs	Small pyroclastic flow moving down northeast chute	
3/6/06	1947 to 2347	Burr Point camera photographs	Incandescence at summit and north and northeast flanks	Flows travel farther down flanks than during the morning of 3/6/06
3/6/06	22:39:02	ASTER nighttime thermal	Strong thermal anomalies at summit and north and northeast flanks	Light clouds
3/7/06	daylight hours	Mound camera photographs	All visible flanks covered in fresh ash	
3/7/06	daylight hours	Burr Point camera photographs	Ash emissions; north lava flow steaming; still no lava flow down northeast chute	Clear weather
3/8/06	1932 to 2002	Burr Point camera photographs	Incandescence at summit and north and northeast flanks	Clouds partially obscure lower flanks

**Table 1.** List of observations and data used to compile deposit chronology.—Continued

Date	Time (AKST unless noted)	Image type or eruptive event	Observation	Comments
3/9/06		Overflight photographs	Active block-and-ash flows from summit and northeast lava-flow front; northeast lava flow more active than north lava flow; entire northeast sector blanketed by light ash (coignimbrite)	Strong backlight on new deposits, unable to see how far northeast lava flow has progressed down chute
3/9/06	Evening/night	Burr Point camera photographs	Clear views of incandescent areas, including margins of northeast lava flow	
<b>3/10/06</b>		<b>Strongest effusive pulse begins</b>		
3/10/06	0828, 0830, 0859	Mound camera photographs	Block-and-ash flows moving down north and northeast flanks	
3/10/06		Overflight and fieldwork photographs; FLIR	Clear views of both north and northeast lava flows; active block-and-ash flows down east chute and from front of northeast lava flow	Excellent photos and FLIR shot of growing lava flows
3/13/06	Daytime	Burr Point camera photographs	Northeast flow has reached its final length	
3/13/06	22:45:18	ASTER nighttime thermal	Thermal data show extents of the north and northeast lava flows and delineate the hottest areas within them; match up well with low-light camera images from the same night	Clear
3/14/06	Early morning	Low-light camera in Homer	Incandescence, block-and-ash flows	
3/15/06		Fieldwork photographs; FLIR	Both north and northeast lava flows thickened and lengthened compared to 3/10/06; rockfall activity and ash emission diminished	Clear views
3/15/06		Mound camera photographs	Comparison between these and March 10 photos shows advance of northeast lava flow	
3/15/06		Strongest effusive pulse ends		
3/16/06		Overflight photographs	No major changes from last observation	Poor viewing conditions
3/22/06		Overflight photographs	No major changes from last observation	Clear views but images are mostly backlit
3/26/06		Overflight and fieldwork photographs; FLIR	No major changes from last observation; lava-flow fronts still hot, no significant temperature changes	
4/5/06	22:51:30	ASTER nighttime thermal	Summit and deposits still warm	Clear view
4/6/06		Overflight and fieldwork photographs; FLIR	Lava-flow fronts cooler; flow tops similar when compared to previous surveys; lava-flow dimensions unchanged; fumarole/vent atop dome very hot (650°C)	Fresh snow has covered many deposits
<b>4/8/06</b>	<b>1635 to 1708 AKDT</b>	<b>Two rockfall signals seen in seismic data</b>		
4/11/06		Overflight photographs	Small debris field on west side of north lava flow and narrow spokelike ash-fall deposit on northwest flank, both likely result of 4/8/06 rockfall(s)	
<b>4/17/06</b>	<b>1656 to 1732 AKDT</b>	<b>Rockfall signals seen in seismic data</b>		
4/18/06	~1430 AKDT	High-magnification photos from Homer	Intense steaming at summit and upper north flank	Photographs taken through binoculars by Dennis Anderson
4/19/06		Overflight photographs	Dark, sinuous debris deposit along west side of north lava flow (Pba) and spokelike ash-fall deposit on west flank	Both likely from April 17 rockfalls
4/27/06	12:37:30 AKDT	ASTER daytime visual and thermal		Partly cloudy with high cirrus clouds over east part of island

**Table 1.** List of observations and data used to compile deposit chronology.—Continued

Date	Time (AKST unless noted)	Image type or eruptive event	Observation	Comments
5/12/06		Airphotos	No changes	Good views of summit and flanks; no orthophoto made
5/13/06		Fieldwork photographs; FLIR	North-south linear trend of fumaroles and mineralization at summit; scarp along west side of north lava flow that fed April rock avalanches; images of all flowage deposits; summit vent cooled to 428°C	Clear summit views; rock sampling
5/16/06	22:45:16 AKDT	ASTER nighttime thermal	Summit and deposits still warm	Clear view
5/23/06		Overflight photographs	Good views of summit that show individual lava lobes	
<b>5/26/06</b>	<b>0106 to 0748 AKDT</b>	<b>Rockfall signals seen in seismic data</b>		
5/26/06		Mike Byerly photographs	Sequence of six photographs shows rock avalanche	Taken from boat north of island
5/26/06	0638, 0653, 0708 AKDT	Burr Point camera photographs	Two images: first just shows start of avalanche, second shows large ash cloud	
5/29/06	12:37:25 AKDT	ASTER daytime visual and thermal		Clear image
6/2/06		Overflight photographs	Dark debris deposits along west side of north lava flow	Likely from May 26 rock avalanches
7/12/06		Airphotos and orthophoto		Orthophoto used as base for 2006 geologic map (plate 1)
9/30/06	1630 AKDT	Citizen photographs from Homer	Strange, possibly meteoric cloud observed halfway down north flank	
<b>10/1/06</b>	<b>0750 to 0915 and 2116 to 2145 AKDT</b>	<b>Lahar(?) signals seen in seismic data</b>		
10/12/06		Overflight photographs	Pink, braided flow deposits atop lower parts of 2006 deposits on north flank	
10/15/06		Overflight photographs	Pink, braided flow deposits atop lower parts of 2006 deposits on north flank	

Commercial vertical aerial photography was obtained on several occasions throughout the eruption (table 1). Photographs from January 4, February 21, and July 12 were processed commercially to create orthophotos (fig. 2). Photos of the whole island were acquired at 1:36,000 scale, and during each flight a single flight line over the summit yielded photos at 1:12,000 scale. The digital orthophotos were produced at a resolution of 0.5 m/pixel. For features observed only on nonorthorectified photos, the vertical airphotos were digitally scanned at a high resolution, georeferenced to the January 4 base map, and optimized for the area of interest. Orthophoto base maps were supplemented by a 10-m-resolution digital elevation model (DEM) of the island generated in 1990.

Remote automated cameras provided time-stamped images of the volcano during the eruption (Paskievitch and others, this volume). Images from the cameras at the informally named “Mound” on the volcano’s east flank and at Burr Point at the northernmost coastline (fig. 3) often provided important information about event timing when no other data were available (figs. 4, 5).

Thermal imagery was obtained weekly or biweekly during the main phases of the eruption using Forward-Looking Infrared Radiometer (FLIR) cameras (Wessels and others, this volume). The primary FLIR unit is a gimbal-mounted camera that mounts to the underside of a helicopter. FLIR images were often useful in determining the outline of new features in low light or partially steamy conditions and also in making preliminary determinations of the character of deposits based on temperature. In addition, Advanced Spaceborne Thermal Emission and Reflection Radiometer (ASTER) and Hyperion satellite imagery provided emplacement timing and temperature information for certain deposits (Wessels and others, this volume).

We undertook a 3-week-long field campaign in August 2006, after the cessation of eruptive activity. During this time, we field checked deposits that had previously been mapped only from imagery; determined stratigraphic relations; collected samples for petrology, component studies, and grain-size analysis; and measured deposit thicknesses, where possible.

Before and during the eruption, numerous geophysical instruments were installed on the island by AVO, as well as by

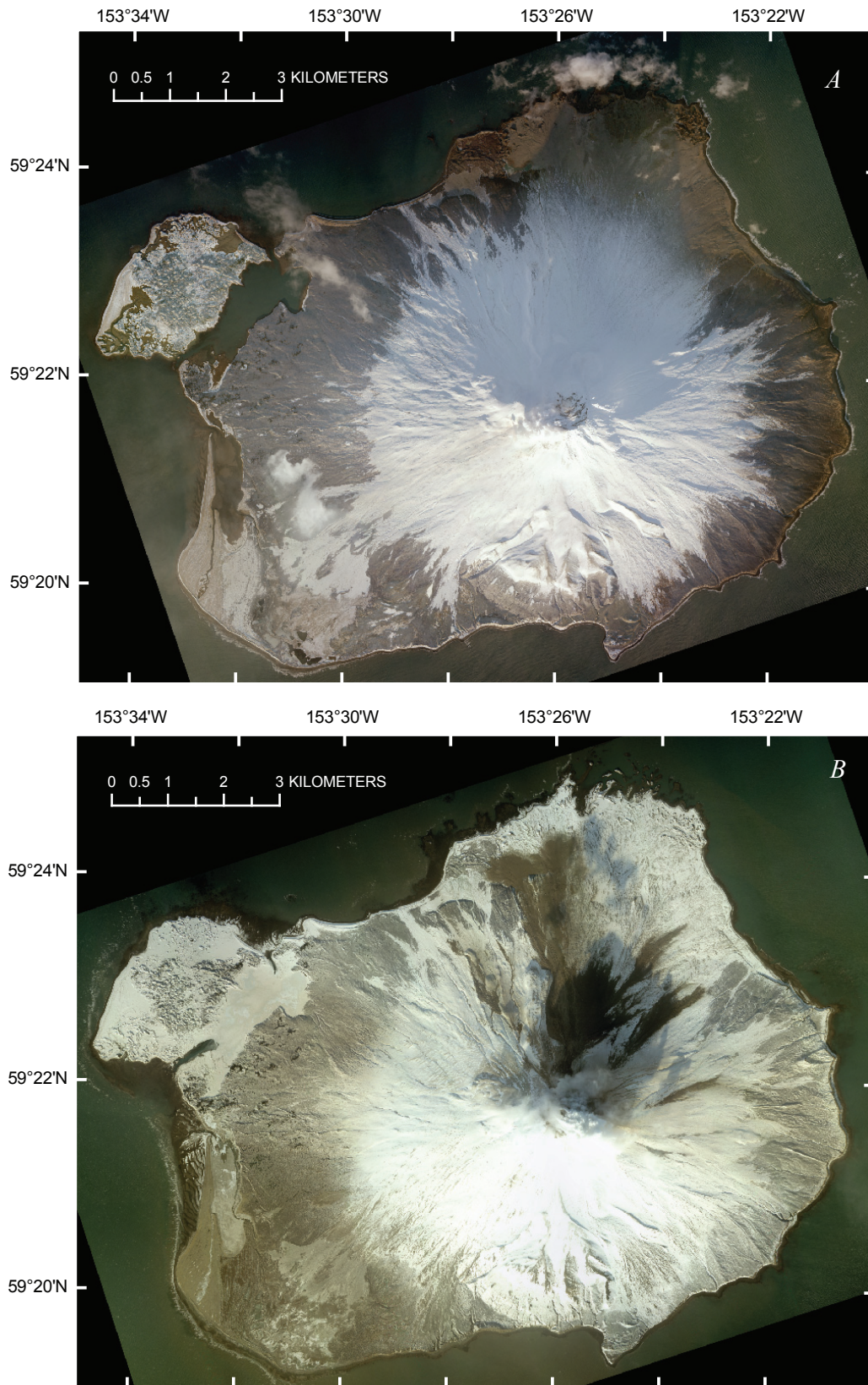


**Figure 2.** Orthophotographs of Augustine Island from *A*, January 4, 2006; *B*, February 22, 2006; and *C*, July 12, 2006. The projection is UTM Zone 5 and the datum is WGS 84.

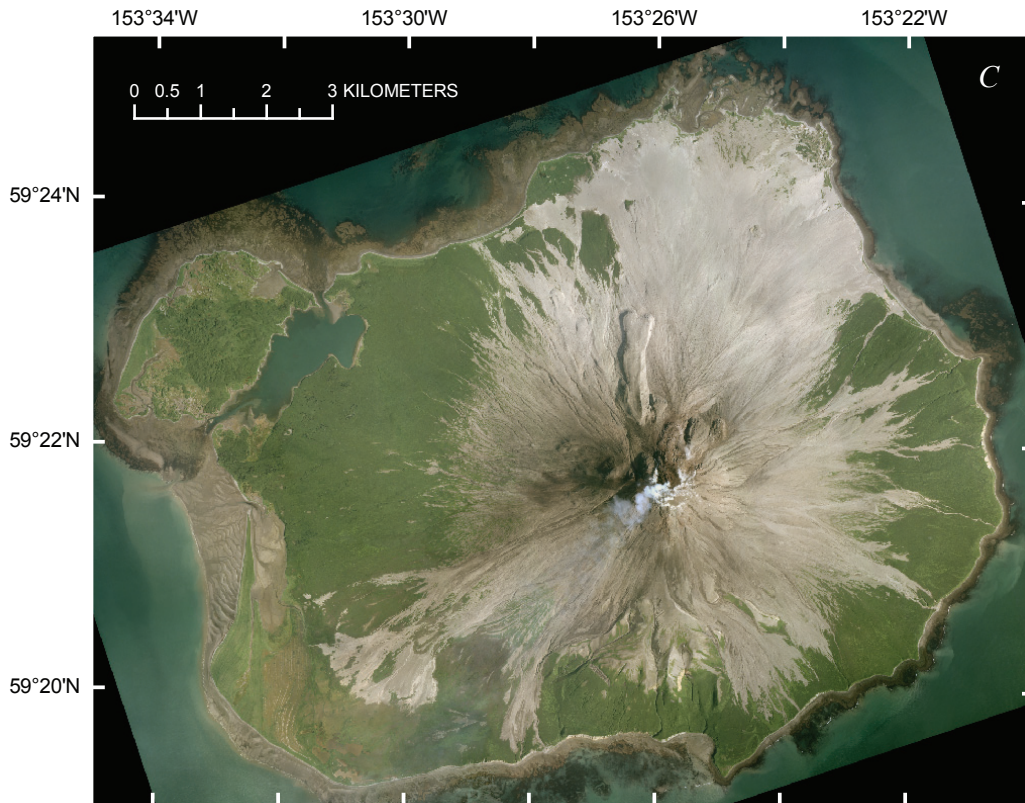


Figure 2.—Continued.

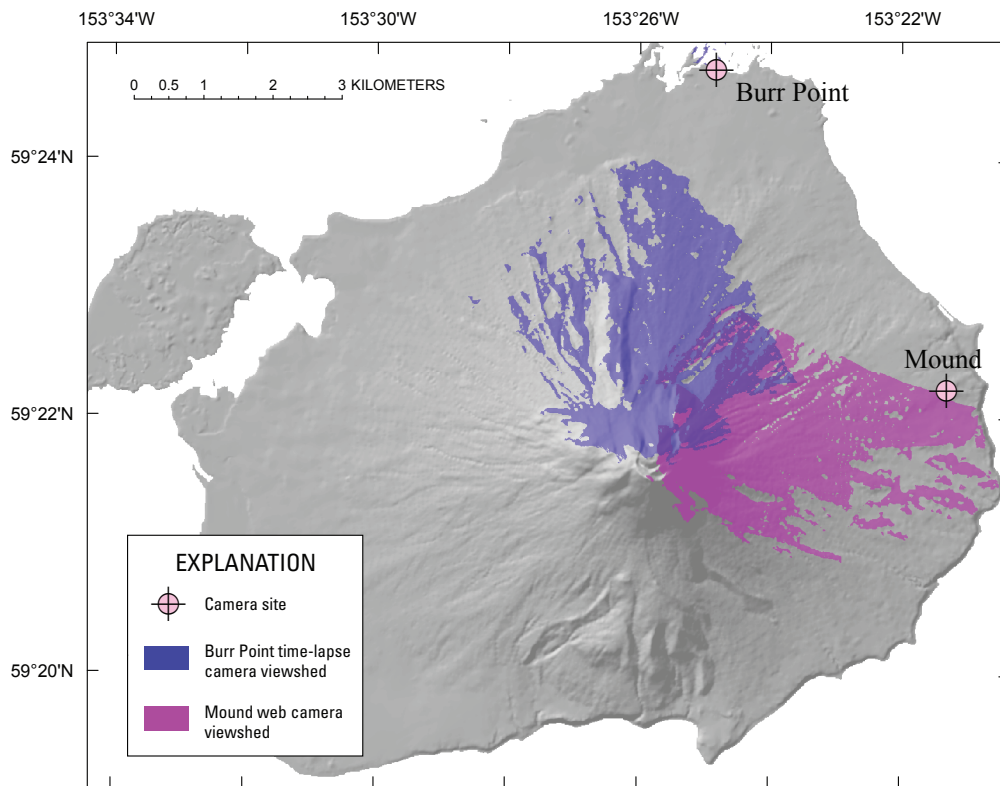
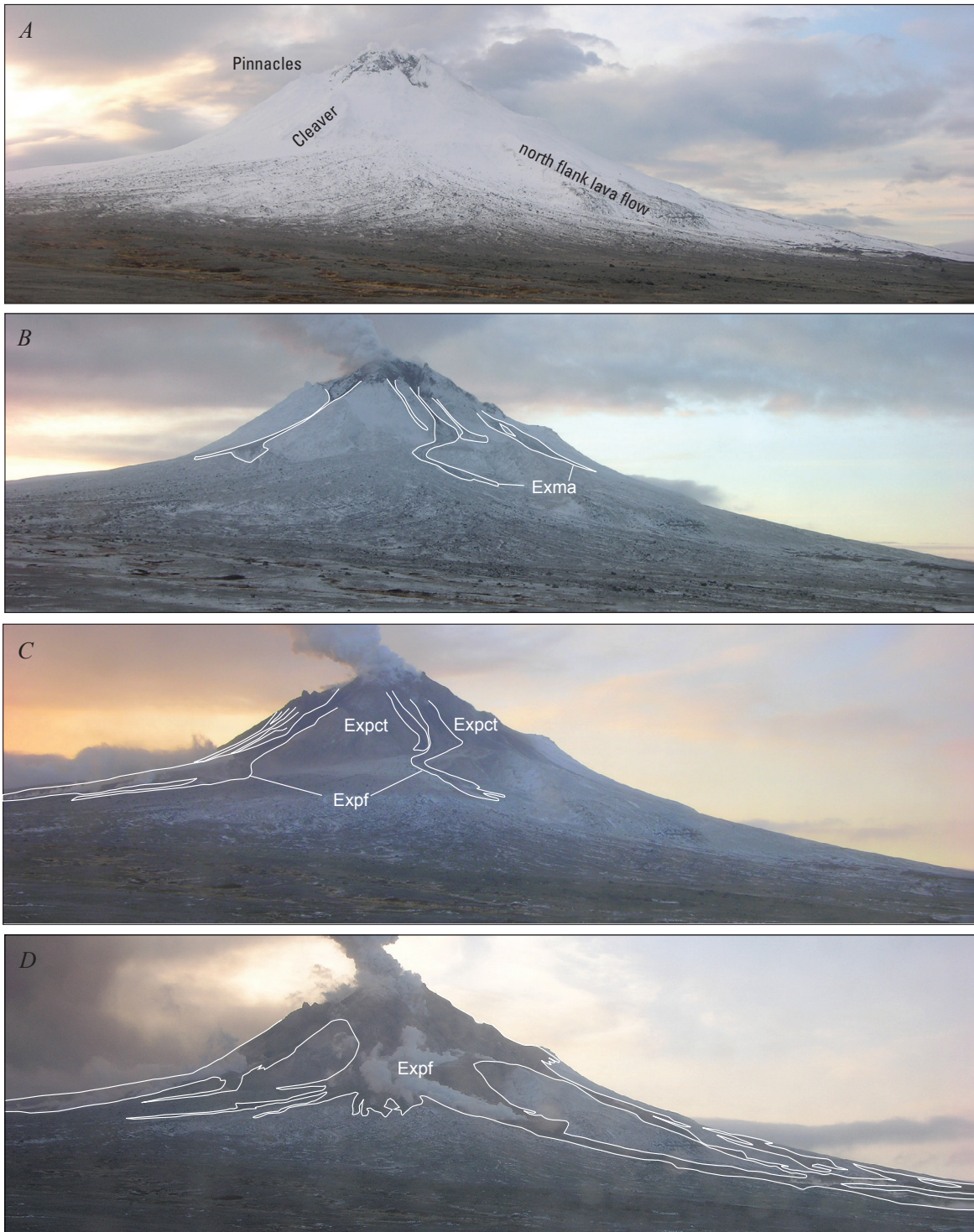


Figure 3. Shaded relief map showing location of on-island cameras and their viewsheds. Digital elevation model from 1990.



**Figure 4.** Views of the north flank of Augustine Volcano from the Burr Point time-lapse camera. All times are in AKST. *A*, 1100 January 5. *B*, 1030 January 12, 2006. Mixed-avalanche deposits formed during events 1 and 2 are outlined. *C*, 1045 January 13, 2006. Pyroclastic flow and current deposits (units Expf and Expct) emplaced during event 4 are outlined. *D*, 1200 January 13, 2006. Pyroclastic-flow deposits emplaced during event 5 are outlined. *E*, 1645 January 13, 2006. Ash cloud from event 6 pyroclastic flow is visible. *F*, January 14, 2006. Pyroclastic-flow deposits newly emplaced during events 7 and 8 are outlined. Other flows from these events may have followed drainages recently filled by previous flow events and, therefore, were not recognized. *G*, February 28, 2006. The Rocky Point pyroclastic-flow deposit (RPpf), pyroclastic-flow deposits (Cpf) from the continuous phase (January 28–31), and the north lava flow (Eflf), which began growing at the end of the continuous phase, are outlined. *H*, May 23, 2006. Lava flows (Eflf) and block-and-ash-flow deposits (Efba) are outlined.

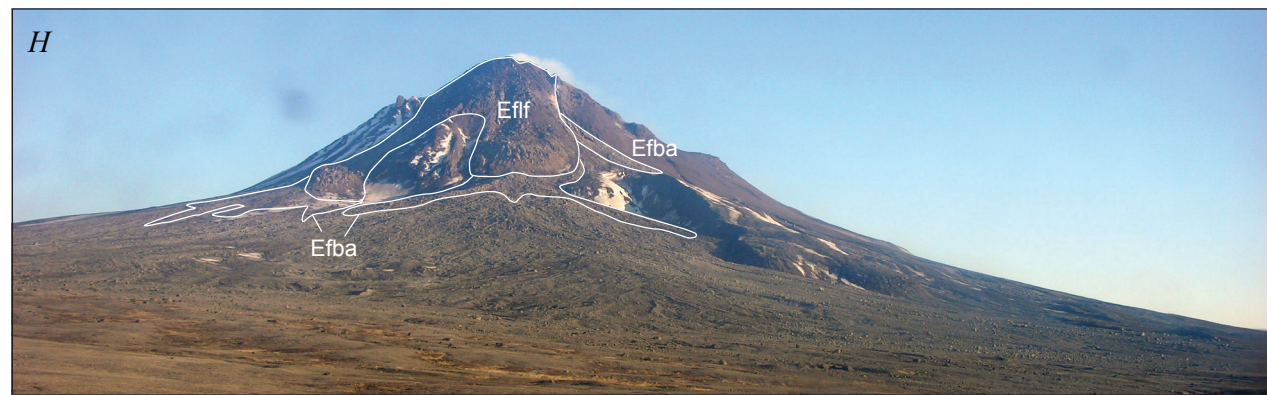
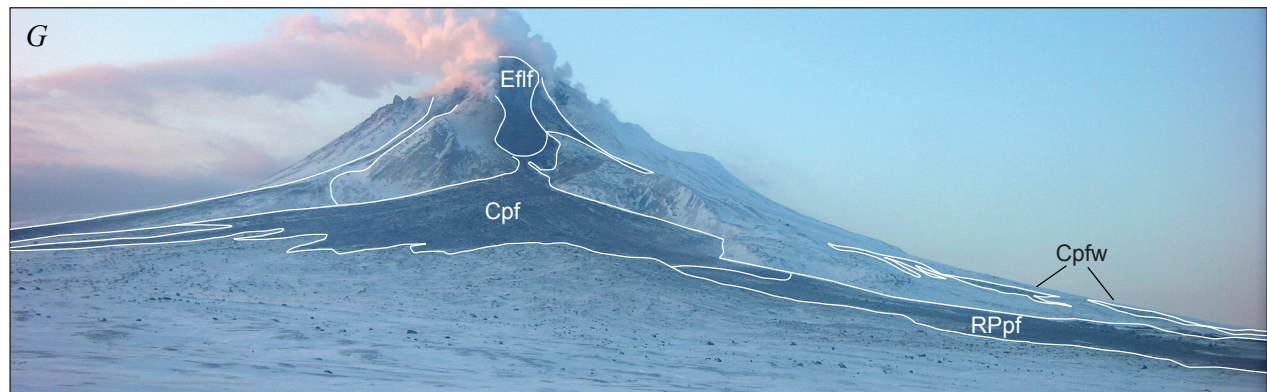
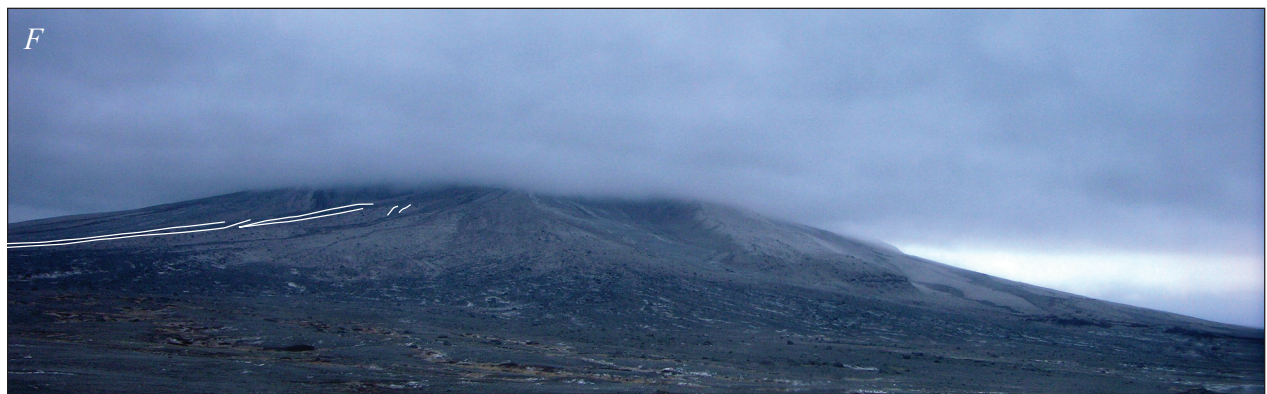
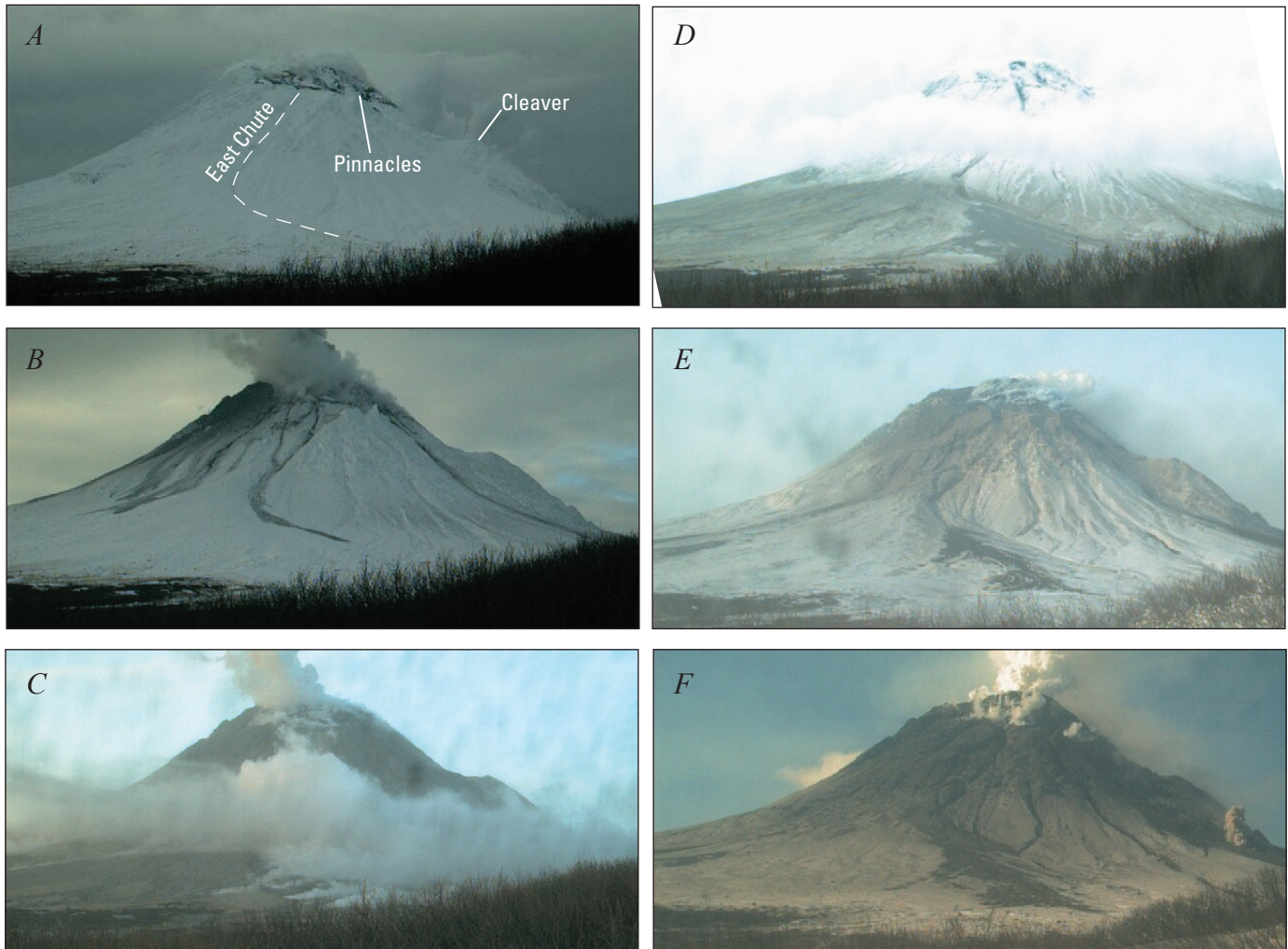


Figure 4.—Continued.



**Figure 5.** Views of the east flank of Augustine Volcano from the Mound web camera. *A*, January 9, 2006. *B*, January 12, 2006. Mixed-avalanche deposits from events 1 and 2 are visible. *C*, 1106 AKST January 13, 2006. Pyroclastic-flow deposits from events 3 and 4 are still steaming. *D*, January 16, 2006. Pyroclastic-flow and ash-fall deposits from events 3–8 blanket the lower flanks; the upper edifice is coated in new snow. *E*, February 8, 2006. The new steaming dome is visible at the summit. Thickest deposits from events 3 through 8 are still warm and snow-free in the east chute (left center) and on the southeast flank (bottom center). *F*, March 15, 2006. Summit dome has enlarged, and northeast lava flow has reached its final length; note small rockfall/block-and-ash flow at its toe.

the National Science Foundation Earthscope/Plate Boundary Observatory. These include a permanent network of short-period seismometers, a temporary network of broadband seismometers in place from December 20, 2006, to August 2006 (Power and Lalla, this volume), and a network of continuous GPS (CGPS) stations installed in 2004 (Pauk and others, this volume). CGPS provided information about edifice inflation and deflation (Cervelli and others, this volume), and the seismic network detected volcano-tectonic and long-period earthquakes, explosion signals, and emergent, cigar-shaped seismic signals associated with the movement of material over the ground surface (McNutt and others, this volume; Power and Lalla, this volume). The latter were particularly useful in

the context of this study to help determine the emplacement locations of several flowage deposits. In addition to the invaluable data they provided while operational, the destruction of several stations recorded the timing of flow emplacement, making them almost as valuable in their demise.

While geophysical data are almost always recorded in UTC (Universal Time, Coordinated), we use Alaska Standard Time (AKST) throughout this paper unless noted, because it better correlates with the more common visual observations described herein. To convert AKST to UTC, add 9 hours. Alaska Daylight Time (AKDT), which is in effect annually after March 21, is 1 hour later than AKST. To convert AKDT to UTC, add eight hours.

**Table 2.** Explosive-phase events and associated flow behavior.

[Locations of seismic stations are shown on fig. 8]

Event No.	Date (2006)	Onset time (AKST)	Duration (mm:ss) <sup>1</sup>	Long coda <sup>2</sup>	Broadband delayed pulse <sup>3</sup>	Seismic station destroyed	Flow direction	Pyroclastic flow	Lahar	Mixed avalanche
1	1/11	0444	1:18	AUW			W			Upper flanks
2	1/11	0512	3:18	AUE	AU12, AU14		NW–E			Upper flanks
3	1/13	0424	11:00	AUE	AU14	AUP	ENE	Likely	Likely, to coast	Likely
4	1/13	0847	4:17	AUE	AU14		ENE	Confirmed, camera	Likely	Possible
5	1/13	1122	3:24	AUW	AU12		NNW	Confirmed, Burr Point camera	Likely, to coast	Likely, to coast
				AUL			N	Confirmed, Burr Point camera	Likely, to coast	
				AUE	AU14		E	Confirmed, Mound camera	Likely, to coast	
6	1/13	1640	4:00	AUE	AU14		E,NE	Confirmed, Mound camera	Confirmed (small), Burr Point camera	Likely
							N			
7	1/13	1858	3:00	AUW	AU12		NNW	Likely	Likely	Probable
				AU14			NE	Likely	Likely	
					AU13		SSW,SSE?	Likely	Likely	
8	1/14	0014	3:00	AUW	AU12		NW	Likely	Likely	Probable, moderate
				AUE	AU14		ENE	Likely	Likely	
					AU13		SSW, SSE?	Likely	Likely, to coast	
9	1/17	0758	4:11	AUE			ENE	Possible	Confirmed, over-flight photos	Likely
				AUW			WNW	Likely		
					AU12		NW	Likely		
10	1/27	2024	9:00		AU15		SW		Likely	Possible
					AU12		WNW			
11	1/27	2337	1:02		AU14		E	Possible	Confirmed, large	Possible, small
						AUL, AUH	N			
12	1/28	0204	2:06	AUW	AU12		N, WNW	Likely	Likely	Likely
				AUE	AU14		E			
13	1/28	0742	3:00	AUW			N, WNW	Likely		

<sup>1</sup>Reported durations were measured at seismic station Oil Point, 30 km northeast of Augustine Volcano.<sup>2</sup>Long coda indicates explosion/flow signals with extended durations that were detected at seismic station(s). Modified from McNutt and others (this volume).<sup>3</sup>Broadband delayed pulse indicates that secondary, high frequency signals were detected on broadband seismometers after the initial signal.

## Volcanic Activity And Resulting Deposits

Similar to recent eruptions of Augustine Volcano, the 2006 activity began with a series of short, discrete explosions, followed by an interval of nearly continuous but less energetic explosive activity that tapered to lava effusion. After a 3-week-long hiatus, effusive activity resumed in March to produce two lava flows. This sequence and the naming of three phases

(explosive, continuous, and effusive) was generally established during the eruption and described in Power and others (2006) and only slightly refined here (fig. 1; table 1).

### The Explosive Phase—January 11–28

Discrete explosive events, each several minutes long, occurred during a 17-day period from January 11 to January 28.

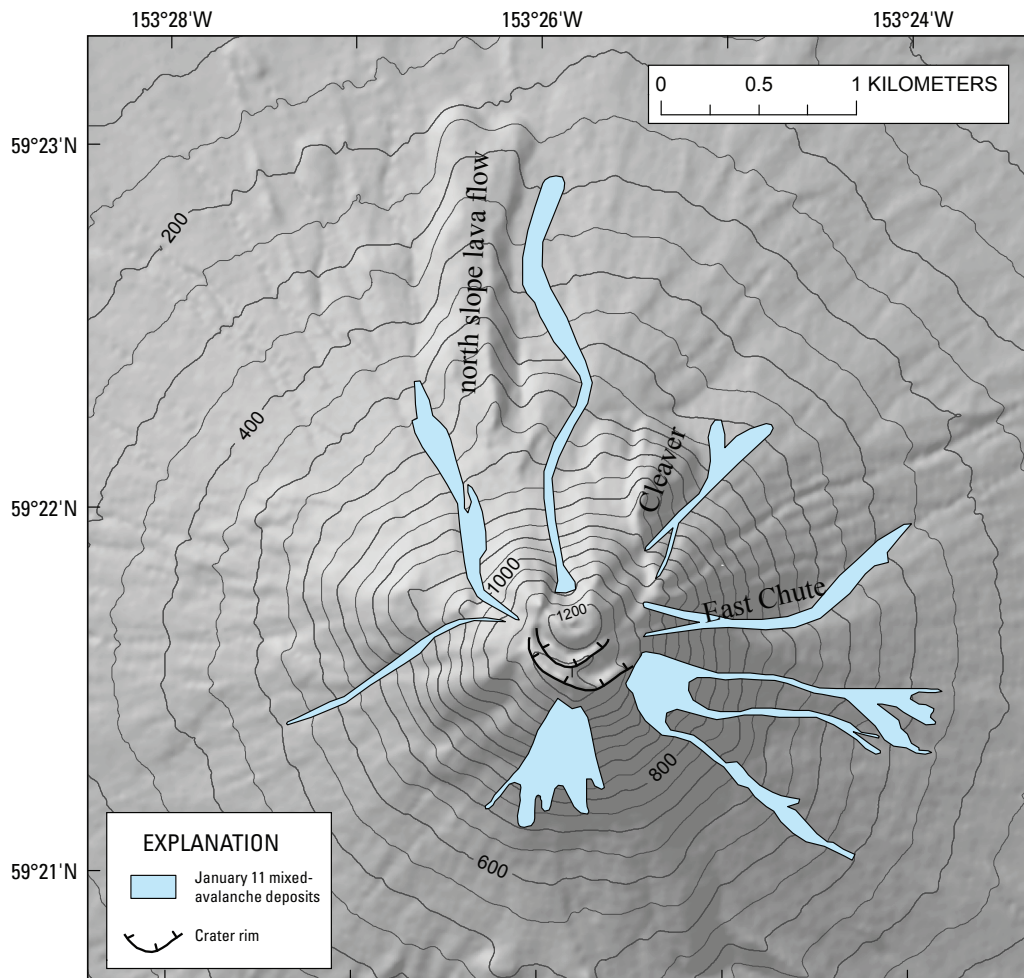


**Figure 6.** Map showing distribution of mixed-avalanche deposits that formed during explosive events 1 and 2 on January 11, 2006. These deposits were covered by later events; their locations are approximate. Contours show pre-2006 topography; contour interval is 50 m.

This time period is termed the “explosive phase” and individual events have been numbered 1 through 13 (Petersen and others, 2006; Power and others, 2006; table 1). Each event is best characterized by its seismic signal, which for many events records energy released during the initial ejection of material from the vent followed by ground shaking caused by movement of pyroclastic and other flows over the ground surface (McNutt and others, this volume). Aerial surveillance on January 12, 16, and 18; time-lapse photography; and seismicity constrain emplacement of pyroclastic flows during the sequence of explosive events. Seismic signals from stations downslope of flows or beside flow paths include 10–30-minute-long, high frequency, cigar-shaped codas and increase in amplitude on temporary broadband stations 10–20 minutes after explosions (table 2). Broadband stations downstream of flows show increased seismicity as much as 20 minutes after initial explosion signals. Such distinctive signals on instruments below or next to flows and their absence in other quadrants indicate pyroclastic-flow directions (McNutt and others, this volume). Between the explosive events, seismicity and

visual observations show that lava effusion formed at least three small lava domes at the summit. In this section we describe the individual explosive events and their resulting deposits, as well as the lava domes effused during more quiescent intervals.

### January 11: Explosive Events 1 and 2

At approximately 1530 AKST on January 10, a strong swarm of volcano-tectonic (VT) earthquakes began, culminating in two explosions at 0444 and 0512 AKST early in the morning of January 11 (table 1). These explosions, events 1 and 2, were 1 and 3 minutes long, respectively, as recorded seismically (table 2). They produced ash plumes that reached heights greater than 9 km asl and moved to the north and northeast of the volcano (Bailey and others, this volume; Schneider and others, 2006). Ash fragments sampled during on-island field work on January 12 are primarily dense or weathered, suggesting that these explosions did not release juvenile magma (Wallace and others, this volume).

An overflight of the volcano on the afternoon of January 11 revealed dark flowage deposits on the snow-covered upper south flank, but much of the rest of the volcano was hidden by clouds. An airplane volcanic gas flight, FLIR helicopter flight, and Burr Point time-lapse photographs on January 12 provided much clearer observations of the new deposits (table 1). Presumably all new deposits viewed on January 12 formed during the January 11 explosions.

The new deposits were present on most flanks of the volcano, extending as far as 2.5 km from the summit and reaching down to 300 m asl (figs. 4*B*, 5*B*, 6). Most were narrow and elongate, followed topographic lows, and ended in multiple lobate flow fronts (fig. 7). They were medium gray, and closer photographs reveal that they consisted of mixed snow, ice, and dark-colored debris; no steaming was observed (fig. 7*B*). Several had dark rills that suggest liquid water may have flowed down the central part of the deposits after the mixed snow and debris had come to rest. The flow deposits on the upper south flank appeared more snow rich than the others and formed a broad sheet rather than individual elongate lobes. None of the deposits appeared to have involved running water that flowed beyond the termini of the snow lobes. None of these deposits were sampled and essentially all were covered by subsequent flows on January 13, 14, and 17. Though not included on the deposit map, they appeared similar to later mixed-avalanche deposits of unit Exma (plate 1).

Seismic data provide some clues regarding flow emplacement during explosive events 1 and 2 (table 2). Each explosion registered as a seismic signal on all island seismometers, but some seismometers also recorded prolonged, broader spectrum waveforms after the actual explosions. These are interpreted to reflect the ground shaking caused by flow of rock and ice over the ground surface in the area near the particular seismometer. For event 1, a somewhat extended signal, or long coda, is evident at seismic station AUW on the west flank. For event 2, a long coda was recorded on seismic station AUE on the east flank. In addition, broadband seismometers AU12 and AU14 (on the northwest and northeast flanks, respectively) recorded delayed broad spectrum pulses after event 2, which likely record the passage of avalanches. These results suggest that most of the flows were emplaced during event 2.

### January 11–12: Dome Growth?

In the 36 hours following events 1 and 2, several sequences of small, regularly spaced VT earthquakes, many with identical waveforms, were recorded at rates as high as 3 to 4 per minute and lasted for several hours (Power and Lalla, this volume). Similar earthquakes, often referred to as clones or drumbeats, have been associated with the emplacement of lava domes at other volcanoes, such as Mount St. Helens (Dzurisin and others, 2005). These earthquakes at Augustine suggest that the effusion of new lava may have begun late on January 11. In addition, subdaily CGPS solutions show that

steady summit inflation ceased at roughly 1800 AKST on January 11; this is interpreted as the result of magma arriving at the surface and relieving pressure within the conduit (Cervelli and others, this volume, fig. 8).

Thermal and visual images acquired during a FLIR flight on January 12 revealed a new vent atop the 1986 dome at the volcano's summit, but no unambiguous new lava was observed (Wessels and others, this volume, fig. 6*D*). Later in the eruption, however, juvenile lava was observed without a distinctly strong thermal signature. There may, then, have been new lava at the surface on January 12, but it was not recognized thermally or it was visually hidden by ash and steam. If a dome did form, it was ephemeral and subsequently destroyed by blasts and/or partially covered by younger deposits. Abundant, dense, angular clasts in deposits from ensuing explosions may have been fragments of this ephemeral dome (Vallance and others, this volume).

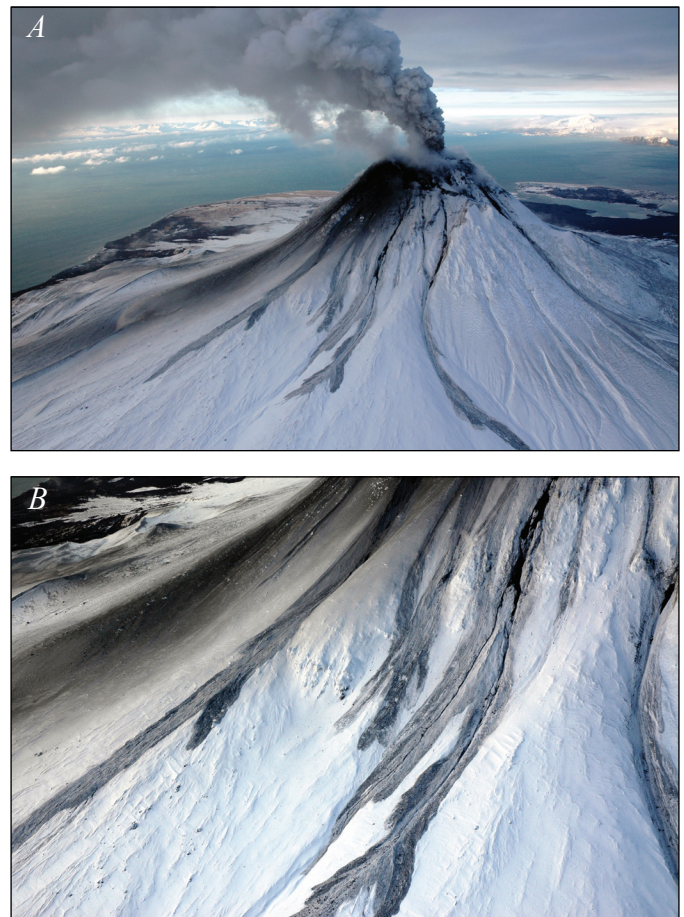


**Figure 7.** Oblique views of January 11, 2006, mixed-avalanche deposits. *A*, Mixed-avalanche deposits on the southeast and east flanks. View to the west. *B*, Detailed view of same deposits. Note streak of discolored snow at upper left that marks ash deposition. Photos by M.L. Coombs, January 12, 2006.

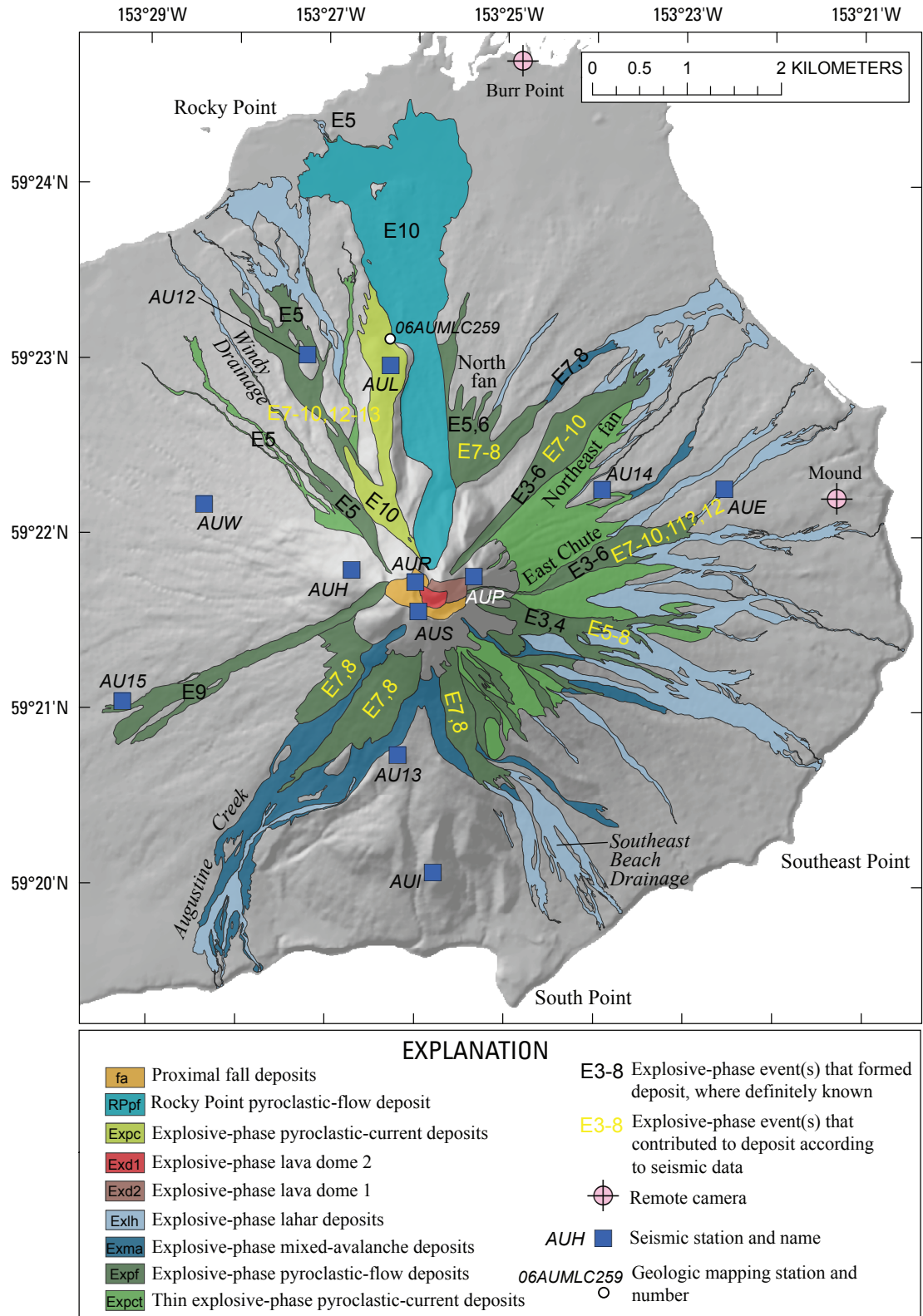


**Figure 8.** Map showing distribution of deposits from the explosive phase. Summit geophysical stations were destroyed during event 3. Station AUE recorded particularly strong seismic signals during events 3 and 4, thought to indicate that these events produced larger flows to the east (McNutt and others, this volume). Station AUL was destroyed during event 10, and debris from the station was found within a pyroclastic-flow deposit at station 06AUMLC259.

## January 13 and 14: Explosive Events 3–8

A second series of six powerful explosions (events 3 through 8), ranging in duration from 3 to 11 minutes, occurred in a roughly 20-hour period between 0424 AKST January 13 and 0014 AKST January 14, as recorded by seismometers and an on-island pressure sensor (Petersen and others, 2006; Power and others, 2006; McNutt and others, this volume; Power and Lalla, this volume). The explosions produced ash plumes that reached altitudes of 14 km asl (Bailey and others, this volume) and deposited trace amounts of ash on the Kenai Peninsula communities of Homer and Port Graham (Wallace and others, this volume).

Explosive events 3 through 8 all resulted in the emplacement of hot pyroclastic deposits on most flanks of the volcano, which take two forms: thin (0–30 cm), laterally extensive (200–600 m wide by as much as 1.5 km long) sheets on the upper flanks, topped by farther-traveled coarse lobate flows (100 to 600 m wide by as much as 3 km long) (Vallance and others, this volume). These deposits have been mapped as two separate units: thin explosive-phase pyroclastic-current deposits (unit Expct) and explosive-phase pyroclastic-flow deposits (unit Expf), respectively (plate 1; fig. 8). Pyroclastic surges likely accompanied the explosions as well but the deposits were poorly preserved. In addition, the emplacement of pyroclastic flows on snow generated areally extensive mixed-avalanche deposits (unit Exma), lahars, and hyperconcentrated flows (unit Exlh; plate 1). These secondary deposits are described in detail in Vallance and others (this volume).

Some of the explosions that occurred on January 13 and 14 were photographed or bracketed by images from the Burr Point and Mound cameras (table 1), allowing us to link emplacement of some flows on the east and north flanks to individual events. The first overflight to the island after events 3–8 was on January 16 (fig. 9). Observers saw that the vegetation-free slopes of the volcano had been uniformly coated in brown ash-fall deposits; this coating somewhat obscured new flowage deposits. Closer inspection revealed that new flows had traveled down many slopes of the volcano and reached the coastline in several places (figs. 8, 9). Most followed tracks of earlier historic flows, but some, such as in the informally named Augustine Creek area (fig. 9A), destroyed vegetation. Later visits to the deposits revealed that pyroclastic flows had been limited to the upper two thirds of the edifice and that the flows that reached the coast were exclusively lahars and hyperconcentrated flows (fig. 8; Vallance and others, this volume).

### Events 3 and 4

Events 3 and 4 occurred before sunrise on January 13 (0424 and 0847 AKST; table 1) and, thus, were not captured by the on-island cameras. The seismic signals for the two events lasted 11 and 4 minutes, respectively. Event 3 destroyed seismic station AUP and continuous GPS AV05 (collocated with AUP), located about 300 m from the volcano's summit

(fig. 8). Both events produced the longest signal durations at short-period seismic station AUE, and the waveforms recorded there have codas indicative of pyroclastic flows (McNutt and others, this volume). Broadband station AU14 shows delayed seismic pulses during both events. These observations suggest that pyroclastic flows from the two events traveled predominantly to the east (fig. 8; table 2).

The event 3 seismic signal at station AUE was particularly long (>30 minutes) and was likely caused, in part, by lahars passing nearby, as well as by pyroclastic flows upslope (McNutt and others, this volume).

Due to darkness, no imagery is available to discriminate between flows emplaced during event 3 or event 4. The first image available after sunrise on the morning of January 13 from the Burr Point camera, at 0900 AKST, shows gray-brown ash clouds on the northeast and east flanks. Those ash clouds were the result of event 4, which began 13 minutes prior (table 1). A series of images from the Burr Point camera from 0915 to 1115 AKST show the ash clouds dissipating and new, fragmental steaming deposits on the northeast and east flanks (fig. 4C). No new discrete deposits were visible on the northwest flank, but the entire snow-covered upper northwest flank had been dirtied by either ash-fall deposits or thin surge or flow deposits. This blanket likely correlated to widespread pyroclastic-current deposits, recognized during August 2006 field work, that compose unit Expct (plate 1; fig. 8; Vallance and others, this volume). The results of events 3 and 4 on the south and west quadrants of the volcano are unknown but likely minor because of the absence of seismicity there.

### Event 5

After a two-and-half-hour lull, event 5 began at 1122 AKST on January 13 and lasted for 3 minutes, 24 seconds. The first Burr Point image after this event, at 1130 AKST, showed an ash cloud rising from the summit and the east flank, while ash and steam shrouded the upper north flank (table 1). Steam and ash were visible rising from discrete tracks on the upper north and northwest flanks and along a single track on the lower north-northwest flank. By 1145 AKST, much of the ash and steam had cleared from the summit area, but a dark-gray cloud remained above the summit and east and southeast flanks. New discrete flow lobes were visible on the upper north and northwest flanks, as well as much farther down towards informally named Rocky Point (fig. 4D). A single flow was captured moving down the upper north flank. By 1200 AKST, the upper flanks were clear of steam and ash, though the lower east-southeast flank was still obscured in ash. Discrete flowage deposits were steaming on the upper north flank.

Seismicity during event 5 corroborates visual evidence. North and northwest of the volcano, stations AUL and AU12 both responded to flows during event 5 but not during earlier events. Because these were the first widespread pyroclastic flows of the sequence to flow north, they probably generated the lahars that moved downstream of the north fan and



**Figure 9.** Explosive-phase deposits on the flanks of Augustine Volcano. *A*, Augustine Creek drainage, looking northeast. Lobate Expf, Exma, and Exlh deposits visible. *B*, View to the northwest. Vegetation-free slopes are covered in snow topped with ash fall. *C*, View to the southwest. Photos by R.G. McGimsey, January 16, 2006.

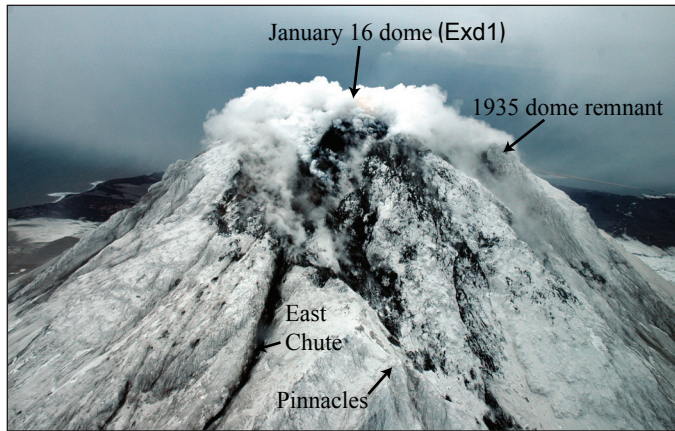


**Figure 10.** Oblique view of Augustine Volcano's summit showing the new lava dome (Exd1), January 16, 2006. View is to the southwest. This dome was later destroyed and/or buried by subsequent eruptive activity. Photo by R.G. McGimsey.

within informally named Windy Creek to the coast (fig. 8). The signal during event 5, in particular, could plausibly include lahars.

#### Event 6

A five-hour lull ensued, followed by event 6 that lasted from 1640 to 1644 AKST on January 13. An image taken from Burr Point at 1645 AKST shows a dark, billowing cloud rising from the east flank and a single pyroclastic flow traveling down the north flank just east of the north flank lava flow (fig. 4E). Photographs from Burr Point taken at 1715 and 1730 AKST show that flows on the north flank from event 6 all followed previous flow tracks; no new mappable areas are covered. A series of images from the Mound camera show a pyroclastic flow or surge descending the east flank toward the camera (table 1; fig. 5 of Paskievitch and others, this volume). As with previous events, we cannot visually determine the extent of flows from this event on the south or west flanks, but seismicity suggests that little material moved in those directions (table 2).

#### Events 7 and 8

Event 7 followed event 6 by 2 hours and lasted from 1858 to 1901 AKST on January 13, and event 8 started 5 hours later and lasted from 0014 to 0017 AKST on January 14. Neither of these events was captured by camera due to darkness. Dawn on January 14 brought overcast skies and clouds that obscured the mountain above approximately 500 m altitude. On the north flank, the Burr Point camera revealed only a couple of new flow deposits that must have formed during events 7 and 8 (fig. 4F).

Based on protracted seismic signals from instruments AU15, AU13, and AUI to the southwest and south of the

volcano, pyroclastic flows and the mixed avalanches and lahars that they generated in Augustine Creek and informally named Southeast Beach Creek (fig. 8) most probably occurred during event 8.

#### January 16: Lava Lobe (unit Exd1)

Following event 8, the volcano entered a 3-day period of relative quiescence. Observers on a January 16 overflight discovered a dark lava lobe at the summit (fig. 10). Satellite images from the same day show that the lobe was roughly 200 m by 160 m and covered  $\sim 27,500$  m<sup>2</sup>; its thickness was unknown but can have been no more than a few tens of meters. It filled the crater that was likely formed during the explosions on January 13 and covered much of the 1986 dome. A satellite image from January 21 shows the same lobe, elongated to the east, but with a crater at the top. Dense, glassy ejecta, prominent in pyroclastic-flow deposits from event 9 on January 17, may be fragments of this dome (Vallance and others, this volume). The lobe likely reached its final size of roughly 275 m by 225 m by event 9 on January 17. Unlike the previous dome of January 11 and 12, no distinctive seismic signals accompanied its effusion (J. Power, oral commun., 2006).

This feature, explosive-phase dome 1 (unit Exd1; plate 1; fig. 8), was only partially covered by later effusion; a portion of it directly above the informally named East Chute remains exposed (fig. 11). It has a smooth surface, morphologically distinct from subsequent lava lobes. A single sample of the dome is low-silica andesite (57.5 weight percent SiO<sub>2</sub>; Larsen and others, this volume).

#### January 17: Explosive Event 9

Approximately 80 hours after event 8, an 8-minute-long explosion, event 9, commenced in darkness at 0758 AKST on January 17 and sent an ash plume to 13 km asl that drifted to the west over the Alaska Peninsula (Power and others, 2006; Bailey and others, this volume).

Images from the Burr Point and Mound cameras from January 18 show that, if any fragmental flows from event 9 traveled down the north or east flanks, they followed the tracks of previous flows from events 3–8. An overflight on January 18, however, revealed a new flow deposit on the southwest flank (fig. 8). This flow traveled approximately 3.5 km from the summit, following a track previously developed by flows from the 1976 and 1964 eruptions (Waitt and Béget, 2009). Satellite images show that event 9 left a large crater in the new lava dome, and observers on the January 18 overflight noted a new field of ballistic blocks on the west and southwest side of the volcano extending to altitudes as low as 760 m (fig. 8). Data transmission from GPS station AV04 on the west flank stopped coincident with this explosion (fig. 8). The pyroclastic-flow deposit from event 9 is rich in dense, glassy clasts (Vallance and others, this volume) that are likely fragments of the new lava dome that had grown since January 14.

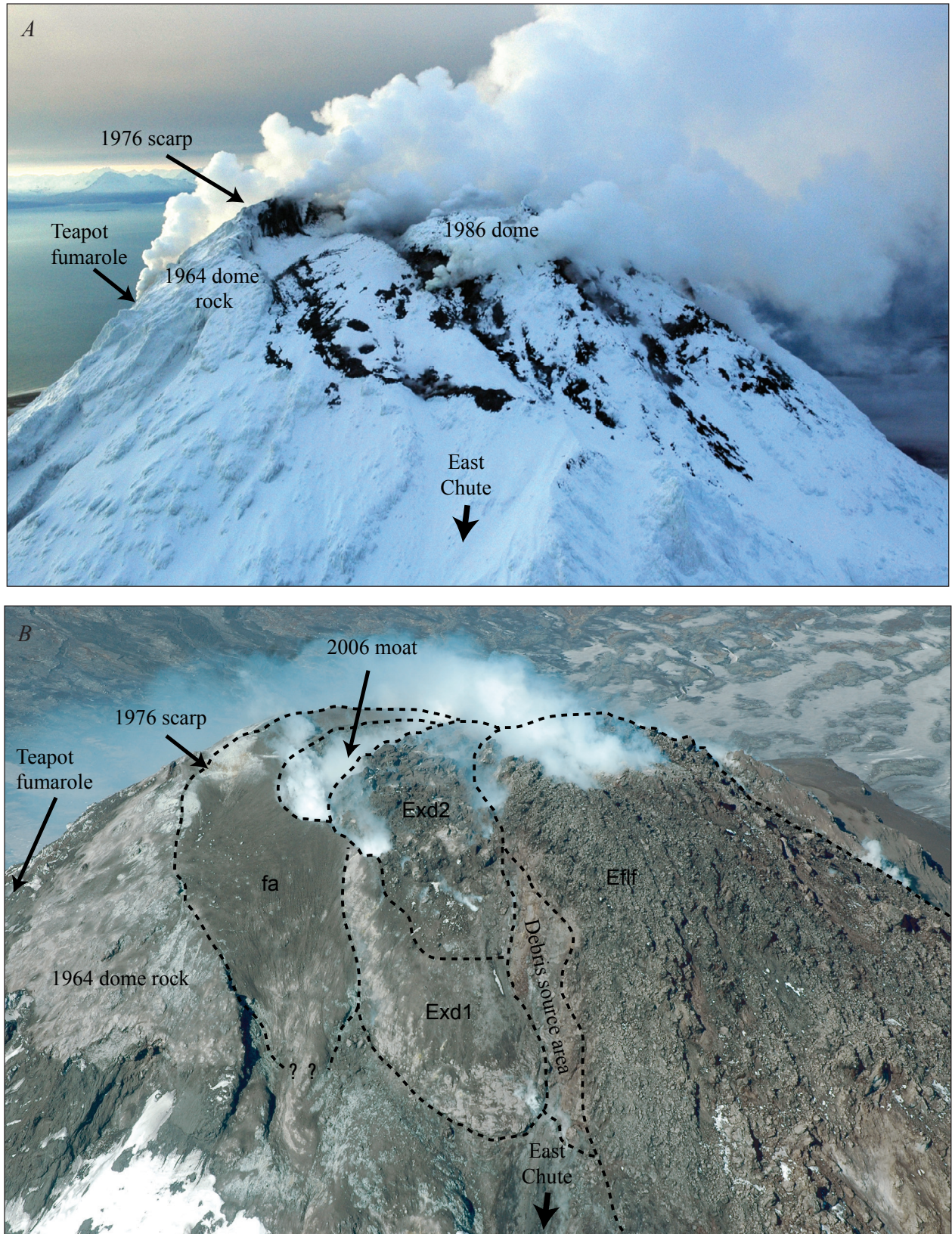


**Figure 11.** Oblique views of Augustine's summit before and after 2006 eruption. Views are to the west. *A*, Photo by K. Wallace, December 22, 2005. *B*, Photo by M.L. Coombs, May 13, 2006. The 2006 deposits are labeled as follows: Exd1, explosive-phase dome 1; Exd2, explosive-phase dome 2; Eflf, effusive-phase lava flows; fa, fall deposits.

### Late January: Lava Effusion (unit Exd2)

Following event 9, Augustine Volcano remained seismically quiet for several days and an overflight on January 24 showed no new deposits on the flanks or changes at the summit. Satellite images from late January show that, at some time, most likely between events 9 and 10 (January 17 to 27), a new lava dome effused at the summit, partially covering explosive-phase lava dome 1 (fig. 8). The lobe is distinct from the earlier lava dome because it is lighter in color and its surface is much more rugged (fig. 11). Samples from this dome are high-silica andesite (62.3 to 63.1 weight percent SiO<sub>2</sub>; Larsen and others, this volume). Explosive-phase lava dome 2 (unit Exd2) was likely partially destroyed during events 10–13 and was also later partially covered by effusive-phase lava. Therefore, its original extent is unknown. The portion of the dome that is still exposed lies within a moat formed by proximal 2006 fall deposits and is to the south of the new main summit dome that reached its final height during the effusive phase.

### January 27 and 28: Explosive Events 10–13

After 10 days of relative quiescence, four explosions ensued in rapid succession: two on January 27 at 2024 and 2337 AKST (events 10 and 11) and two more on the morning of January 28 at 0204 and 0742 AKST (events 12 and 13). These all occurred at night and were initially detected seismically (Power and Lalla, this volume), and the resulting ash clouds were quickly detected by satellite images and radar (Bailey and others, this volume; Schneider and others, 2006). Event 10, the longest of the four at 9 minutes, sent an ash cloud to 10.5 km asl that drifted southeast. The other three ranged from 1 to 3 minutes in duration and sent ash clouds as high as 7.2 km (Schneider and others, 2006).

Because events 10 through 13 were at night, there were no visual or camera observations. The Burr Point camera was not in operation from January 23 to February 24, probably due to extreme weather conditions (Paskievitch and others, this volume). Observation overflights on January 29 and 30 found the island shrouded in ash during continuous-phase activity.

In the absence of visual observations of these events, seismicity and the destruction of geophysical stations provided clues about the accompanying activity. Event 10 destroyed station AUH, high on the volcano's west flank, 7 minutes after the beginning of the event and coincident with the strongest phase of the seismic signal recorded at broadband stations around the island. Event 10 also destroyed station AUL/AV03 near the toe of the prehistoric north flank lava flow (fig. 8). Unfortunately, the precise time of station AUL/AV03 destruction is unknown: the broadband seismometer at AUL had stopped sending data before the beginning of event 10, for unrelated reasons. The last data packet from GPS site AV03 was sent at 0459 AKST, however, 25 minutes before the start of the event (GPS data were transmitted on an hourly

basis). Tellingly, pieces of the station were found within a new deposit below the north flank lava flow at locality 06AUMLC259 (fig. 8). This deposit is map unit Expc (explosive-phase pyroclastic-current deposits) and is mapped separately from other explosive-phase units due to its increased proportion of dense clasts and fines-deficient matrix (fig. 8; plate 1; Vallance and others, this volume). In addition to the different grain-size distribution, the deposit has a lithologic make-up that is transitional between earlier explosive-phase and later continuous-phase deposits—it contains low- and high-silica andesite in approximately equal proportions (Vallance and others, this volume).

In addition to the explosive-phase pyroclastic-current deposit mentioned above, there is evidence that event 10 also generated a second, larger pyroclastic flow. At the Oil Point reference seismic station, 30 km northeast of Augustine Volcano, the event seismic signal lasted 9 minutes (table 2), but its duration was minutes longer at several on-island stations and appears to record multiple flowage events (McNutt and others, this volume, fig. 4). The most plausible candidate to have also formed during event 10 is a 4.8-km-long pyroclastic-flow deposit on the north flank, first observed in an ASTER image from January 31 (Wessels and others, this volume) (fig. 4G; fig. 8). Named here the Rocky Point pyroclastic flow (unit RPPf; plate 1), it appears to have descended the north flank just east of the north flank lava flow before spreading out and filling in a small pond near the toe of the lava flow (Vallance and others, this volume). The deposit immediately overlies the explosive-phase pyroclastic-current deposits mentioned previously and immediately underlies the continuous-phase pyroclastic fan on the north flank. It is lithologically similar to continuous-phase deposits because it contains a high fraction of high-silica andesite clasts (Vallance and others, this volume).

While assigning the Rocky Point pyroclastic flow to event 10 is consistent with stratigraphy, the size of the deposit, the duration of the event 10 seismic signal, the airborne ash record from radar, and the lightning record all provide further evidence that link the two:

5. The Rocky Point pyroclastic flow is the single largest deposit of the eruption, with a volume of roughly  $17 \times 10^6$  m<sup>3</sup> and a length of 4.8 km, thus we expect that the associated seismicity would be the longest flowage-derived signal during the time period when we know the flow was emplaced. Flow velocities of 5–10 m/s would require the emplacement of the flow over 8–16 minutes. For example, the smaller-volume, 3.7-km-long windy pyroclastic flow from the continuous phase (mapped as unit Cpfw) took roughly 7 minutes to come to rest. Between January 24, when observations show the Rocky Point flow to not be present, and the January 31 ASTER image, the longest flow/explosion signal recorded was during event 10.
6. During the continuous phase, the strongest ash signal detected by radar was from the windy pyroclastic flow, suggesting that

the much larger Rocky Point flow was not emplaced during the continuous phase (Schneider and others, 2006).

7. Event 10 produced the greatest number of lightning strikes between January 27 and the end of the eruption, the interval when a lightning-detection unit was operational (Thomas and others, this volume). The high number of lightning strikes can be the result of higher concentrations of airborne ash and/or the presence of additional steam, perhaps created as the Rocky Point pyroclastic flow entered the small pond (S. McNutt, written commun., 2007).

We have little information on the nature of flowage deposits produced during events 11–13 late on January 27 and early on January 28. Event 11 was very brief and it likely produced only minor deposits. The most energetic phases of events 12 and 13 lasted from 1 to 3 minutes, but the seismic signal had a long coda for event 12 at stations AUW and AUE and for event 13 at AUW, suggesting flows may have traveled east and northeast (McNutt and others, this volume). It seems likely that any pyroclastic-flow deposits from these two events are lithologically similar to the Rocky Point flow and to flows of the subsequent continuous phase.

## The Continuous Phase—January 28–February 10

On the afternoon of January 28 at about 1430 AKST, 7 hours after event 13, Augustine Volcano entered a period of more continuous eruptive activity that lasted for 13 days. This period was characterized by (1) essentially continuous ash emission to heights of commonly less than 3,600 m asl, generating a variably ash rich plume, as recorded by satellite images and radar (Bailey and others, this volume; Schneider and others, 2006), (2) emplacement of pyroclastic flows on the north flanks of the volcano, as recorded by cigar-shaped seismic signals (Power and Lalla, this volume) and viewed in overflights, and (3) occasional larger seismic signals, thought to represent more explosive events, associated with ash clouds as high as 4,500–7,600 m asl. Ash fall was reported in Homer and Seldovia during this period (Wallace and others, this volume), 115 and 100 km east of the volcano, respectively. Activity waxed and waned during the continuous phase, as evidenced by variations in the number and duration of flow-related seismic events. The most vigorous activity ended on February 3 and was followed by steady effusion of a new lava dome and flow that lasted until approximately February 10. This entire interval from January 28 to February 10 is termed the “continuous phase” to distinguish it from the punctuated nature of the explosive phase.

### January 28–February 3: Pyroclastic-Flow Emplacement

The early continuous phase resulted in a series of pyroclastic-flow deposits (units Cpf, Cpc, and Cpfw) on the

north quadrant of the volcano (fig. 12; plate 1). These deposits cover an area of 4.9 km<sup>2</sup> and extend as far as 3.8 km from the summit. Several observation flights during the January 28 to February 3 interval provided information about the style of eruption (table 1), though observations of the volcano were hampered by airborne ash and poor weather. Additional evidence for timing of flow emplacement from this period is from seismicity, satellite images, and flow stratigraphy. The Burr Point time-lapse camera was not operational during the continuous phase, but the Mound camera provided several images of the activity during clear weather.

Seven hours after the four discrete explosive events on January 27 and 28 (events 10–13), seismometers recorded a roughly 2-hour period of volcanic tremor beginning at 1431 AKST on January 28. Starting at about 1418 AKST on January 28, coincident with (or slightly preceding) the increasing seismic tremor, Mound camera images revealed an ash-laden, vertically convecting plume that increased in vigor over the afternoon. Images show that no pyroclastic or debris flows or ash were deposited on the volcano’s north flank on January 28.

Beginning at 2200 AKST on January 28, seismic signals, at the rate of 5–10 per hour, first recorded the movement of pyroclastic flows down the flanks. The first visual evidence of flows on the north flank is from 1007 to 1015 AKST on January 29, when the Mound camera showed a thick billowing plume that rose from the summit and moved south and another ash cloud that rose from the north half of the summit and moved down the north flank (fig. 13).

A particularly strong seismic signal was recorded by the network starting at 1118 AKST on January 29. This emergent, broad-spectrum signal lasted for roughly 5 minutes and had the longest duration of any signal during the 13 hours since continuous activity began. Several lines of evidence suggest that it was caused by a large pyroclastic flow on the north flank. In web-camera images from Homer, the top of a wide ash cloud was visible above meteoric cloud tops from 1127 to 1137 AKST. Images from the Mound camera went dark starting at 1126 AKST, suggesting significant ash in the air. An observation flight on January 29 arrived in the vicinity of the island around 1230 AKST. Views of the volcano were hindered by broken clouds below and dense clouds above 2,100 or 2,400 m asl, but observers saw a plume from the summit vent that rose vertically and then turned southward, with ash visible to the south of the island. Observers also noted a prominent ash-and-steam cloud that rose from the upper north flank of the island (fig. 14A); the lower north flank was mostly obscured by clouds and ash. During the viewing period, this ash cloud dissipated, revealing discrete but widespread areas of steaming. A more diffuse, brown-gray cloud that drifted low above the coastline was plausibly a coignimbrite cloud. We cannot identify the exact deposit emplaced during this event, but it is likely one of the longer flow lobes on the north fan that extend down to 50–100 m asl (fig. 12).

For most of the rest of January 29, images from the Mound camera were dark, but by 1547 AKST the view cleared

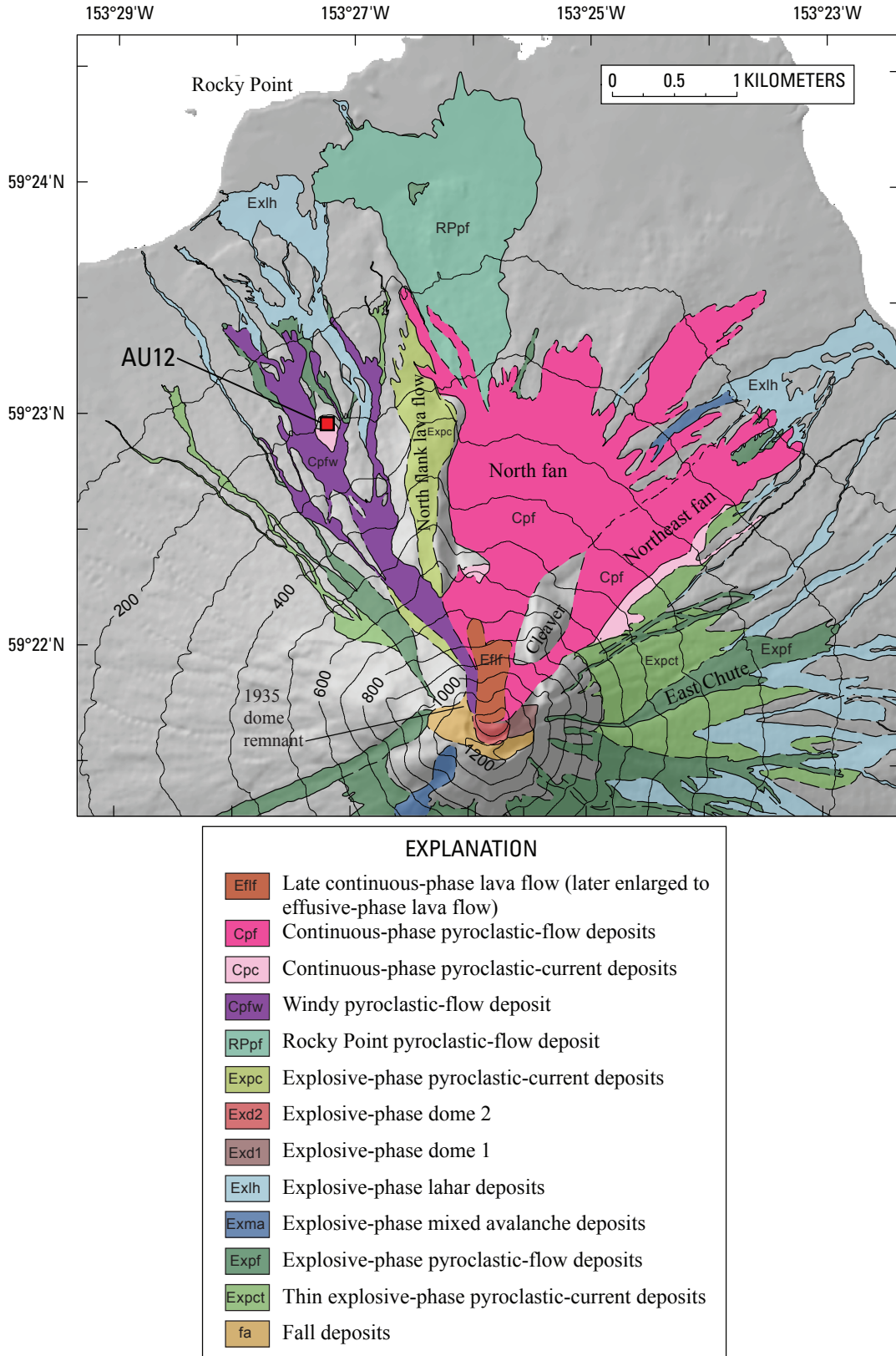


**Figure 12.** Map showing distribution of deposits at the end of the continuous phase (February 10, 2006). The location of broadband seismic station AU12, which was destroyed on January 30, 2006, is shown as a red square. Contours show pre-2006 topography; contour interval is 100 m.

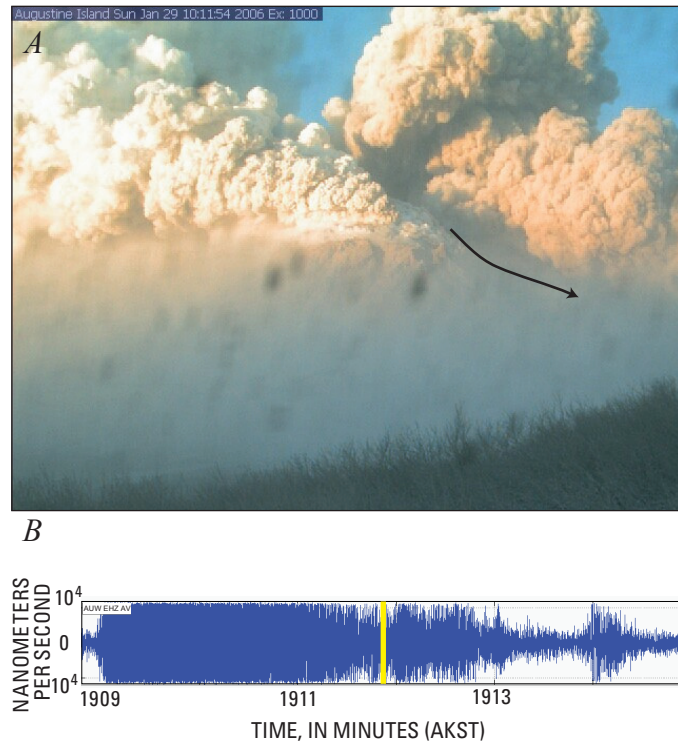


**Figure 13.** *A*, Mound web camera image from 10:11:54 AKST on January 29, 2006, showing intense steaming and likely ash emission from the summit and a small pyroclastic flow on the north flank (path shown by arrow). *B*, Seismic signal from station AUW showing small pyroclastic flow. Time that image was taken is shown by yellow line.

to show a dark cloud moving south and, in a single image, an ash cloud was visible rising from the north flank.

The destruction of a geophysical station recorded the passage of the single largest pyroclastic flow during the continuous phase. Campaign broadband seismic station AU12, on the northwest flank, was destroyed on January 30 at 0329 AKST (figs. 12, 15). We found the destroyed station at the edge of a pyroclastic-flow deposit in the summer of 2006. This braided deposit is named the windy pyroclastic flow deposit (unit C<sub>pfw</sub>; plate 1) and is lithologically identical to other continuous-phase deposits (Vallance and others, this volume). Interestingly, AU12, which was 2.6 km from the summit, was destroyed approximately 4.5 minutes after the start of the flowage seismic signal, yielding an average flow rate of 9.6 m/s. During the 1976 eruption of Augustine Volcano, a series of time-stamped photographs recorded a pyroclastic flow that traveled at 50 m/s on the steep upper slopes and slowed to ~6 m/s as it reached the north coastline (Stith and others, 1977). The flowage seismic signal, which was no longer recorded by AU12 after its destruction, continues for approximately another 3 minutes on nearby broadband station AU11. If we assume that the flow traveled at the slower rate of 6 m/s for the rest of its course on the lower slopes of the volcano, it would have covered roughly 1.1 km in that time,

for a total of 3.7 km. This is the exact length of the windy pyroclastic-flow deposit, suggesting that the entire flow was emplaced during this single flowage event. Radar data for this time interval shows the greatest ash signal seen during the continuous phase (Schneider and others, 2006), which is consistent with the idea that the windy pyroclastic flow was emplaced during a single, large event.

Smaller flowage signals continued to be recorded by the seismic network at a relatively high rate through February 3, though none were as large as the two on January 29 and 30. An overflight midday on January 30 revealed a dense vertical column rising from the summit vent to 4,900 m asl before drifting off as an ash cloud to the northeast for roughly 145 km (fig. 14*B*). The northern portion of the vertical eruption column and the tephra cloud moving to the northeast were brown gray and appeared more ash rich; the central, billowing part of the plume immediately above the vent was lighter colored. No fresh flowage deposits were identified in the southwest and southeast quadrants. An ashy haze that surrounded the slopes of the volcano, especially thick on the north flank, prevented views of the ground surface. During an observation flight on

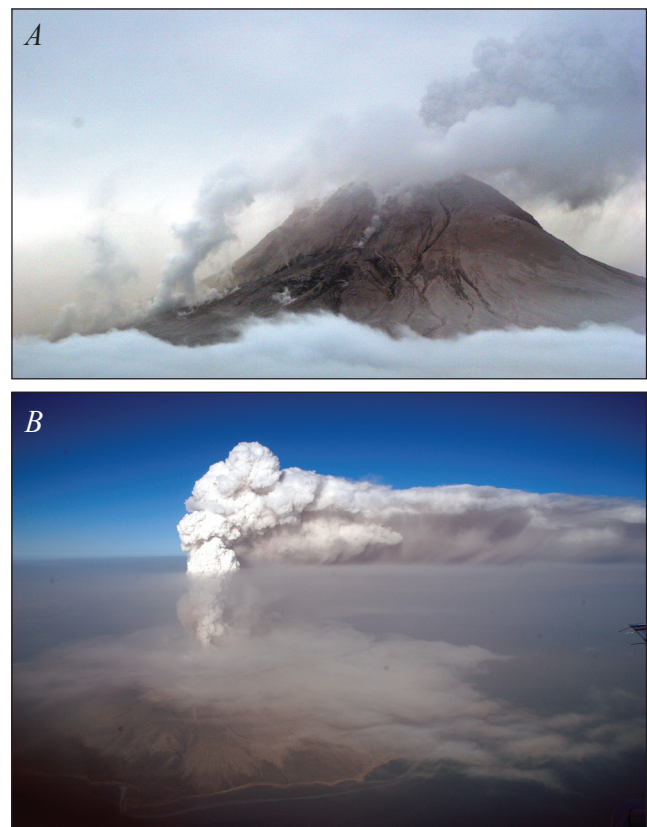


**Figure 14.** *A*, Photograph of the upper north flank of Augustine Volcano, taken by K. Wallace during January 29, 2006, overflight. Steaming flows are visible. *B*, Photograph of Augustine Island, looking north, taken by R.G. McGimsey during January 30, 2006, overflight.

February 3, the volcano was completely obscured by clouds, but observers saw an ash cloud above the volcano that reached to approximately 1,800 m asl. A brown plume was rising from high on the north flank.

Satellite images provided the first direct view of deposits of explosive events 10–13 and the early continuous phase (table 1). An ASTER image from January 31 showed the windy pyroclastic flow, the Rocky Point pyroclastic flow, and the north continuous-phase pyroclastic fan; much of the northeast flank was obscured in the image by a SO<sub>2</sub>-rich plume (Wessels and others, this volume). A Hyperion satellite image from February 2 showed a strong thermal signature from the summit and a thin streak down the northeast chute; these were presumably a summit lava dome and a thin block-and-ash flow deposit (Wessels and others, this volume).

Observers first saw continuous-phase pyroclastic-flow deposits during a FLIR flight on February 8 (fig. 16). The deposits were dark and steaming, contrasting sharply with the surrounding snow-covered flanks. Numerous small pyroclastic flows constructed fans of fragmental debris on the north and northeast flanks. The fans resemble those from 1976 and 1986 eruptions in similar locations. On the northwest flank, the thickest portions of the windy pyroclastic-flow deposit (unit C<sub>pfw</sub>) were visible as braided fingers; thinner and presumably cooler portions were obscured by new snow. Field work during August 2006 revealed that all continuous-phase deposits are light gray and poorly sorted and contain abundant, dense, large, high-silica-andesite blocks that resemble rocks of the second explosive-phase dome (Vallance and others, this volume).

### February 3–10: Beginning of Lava Flow Effusion

The number of flow-related seismic signals tapered off over a period of 24 hours from roughly February 3 to February 4. Seismicity increased again over a 24-hour period on February 5. Beginning around February 3, the ash emission of the

early continuous phase gave way to lava effusion that persisted through February 10, as evidenced by continued rockfall seismic signals, continued deflation as recorded in CGPS (Cervelli and others, this volume), persistent thermal anomalies in satellite data (Bailey and others, this volume), and incandescence at the summit and upper north flank viewed from Homer in early February (Sentman and others, this volume). Lava slowly or intermittently extruded from the summit area became unstable

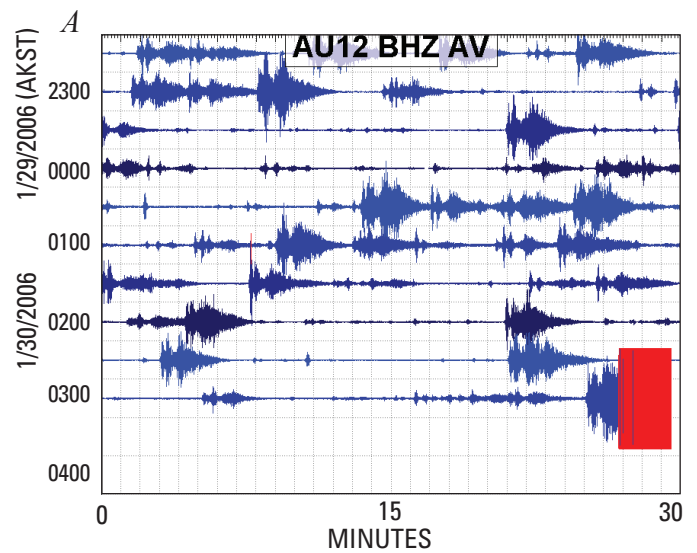


**Figure 15.** *A*, Seismic record showing a series of pyroclastic-flow signals recorded by campaign broadband seismometer AU12 on Augustine Volcano's northwest flank (see fig. 12 for location). The final flow signal ceased at 0329 AKST on January 30, 2006, when the station was overrun by the windy pyroclastic flow. Red rectangle indicates time period when signal strength exceeded the range of the instrument. *B*, Photograph of destroyed seismic station AU12. The data card was still intact and recorded that the station ceased operation on January 30 at 0329 AKST, presumably coincident with the emplacement of the windy pyroclastic flow. Larger boulders predate the 2006 eruption. The flow left only a thin deposit in this area but melted the station casing and much of the equipment. Flow direction was from top to bottom in the image. Adze is approximately 1 m long. Photo by M.L. Coombs, August 10, 2006.

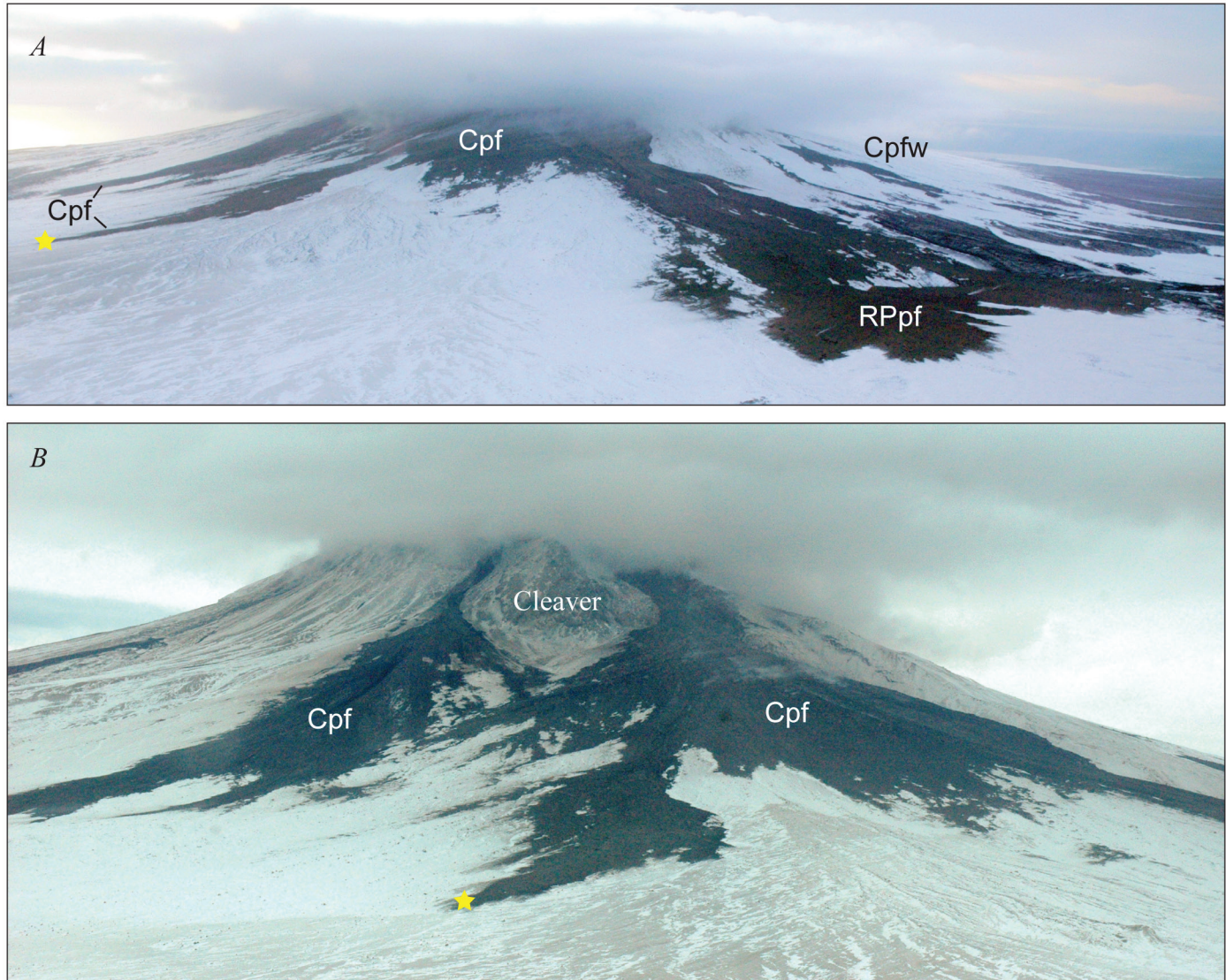


**Figure 16** Photographs of continuous-phase pyroclastic-flow deposits, taken Feb 8, 2006. *A*, View towards south. *B*, View towards southwest. Star shows toe of the same flow deposit in both photos. Photos by M.L. Coombs.

and occasionally tumbled down the flanks as block-and-ash flows and rock falls. These events sometimes generated low-level ash clouds to altitudes of less than 3,000 m asl.

By February 7, satellite images showed that a multi-lobe lava flow had made its way down the north flank. It covered 215,000 m<sup>2</sup> and was roughly 900 m long by 300 m across. The lava progressed down a chute between the 1935 dome remnant and the informally named Cleaver (fig. 12). FLIR and visual observations on February 20 and 24 (Wessels and others, this volume) reveal that, by that time, the north lava flow was approximately 1,000 m long and that it extended from a new, dark, rubbly lava dome that covered the north half of Augustine's summit (fig. 4*F*). Given the lack of seismicity after February 10, we interpret that most of this growth occurred before then.

### Eruptive Hiatus—February 10–March 3

During the period from February 10 to March 3, seismicity was low and no visual evidence exists to suggest that measurable volumes of magma were being erupted. FLIR flights on February 20 and 24 showed few changes had occurred at the summit (Wessels and others, this volume). However, several small explosions were recorded by seismic instruments and by the on-island pressure sensor (McNutt and others, this volume), and scattered rockfalls were recorded seismically. Periods of incandescence seen with the Homer low-light camera (Sentman and others, this volume) and with the Burr Point camera between February 15 and March 1 likely recorded the fracturing and spalling off of the lava-flow front.





**Figure 18.** Photograph of the north flank of Augustine Volcano, taken from Burr Point time-lapse camera on May 13, 2006. Areas of incandescence, color-coded by day, are shown.

### The Effusive Phase—March 3–16

After an apparent pause in eruptive activity throughout the latter half of February, Augustine Volcano resumed activity in March with the effusion of a larger summit dome, renewed growth of the north lava flow, and formation of a new lava flow down the northeast chute, all accompanied by vigorous block-and-ash flows (fig. 17; plate 1). In contrast to the continuous phase, clear weather and lesser amounts of airborne ash allowed thermal, visual, and satellite observations during this phase, which augmented seismic data. During this time, incandescent areas were observed at the summit and extending down the north flank; motion of incandescent blocks and/or flows was also observed. This activity was seen in nighttime images from the Homer camera, the low-light camera (also located in Homer; Sentman and others, this volume), and the Burr Point time-lapse camera (the Mound camera was not turned on at night due to power considerations; Paskievitch and others, this volume).

An increased number of rockfall seismic signals late in the evening of March 3 heralded the beginning of the effusive phase (Power and Lalla, this volume). On March 4, a series of small, localized ash emissions from the summit were captured with the Mound camera (table 1; fig. 5).

Observations of incandescence, though sometimes hampered by cloudy conditions, commenced during the night of March 5 and provided clues about the style of activity and growth of the lava flows and dome (fig. 18). Two types of incandescence were observed by Burr Point and Homer cameras. First, relatively stationary points and regions of incandescence represented exposed, hot parts of the growing lava dome or flows. Second, glowing streaks that moved downslope in subsequent, closely timed images (Sentman and others, this volume) represented block-and-ash flows

shed from the summit dome and from the toes and flanks of the lava flows. These pyroclastic flows descended the north, northeast, and east chutes from the summit and were synchronous with seismic signals (DeRoin and others, 2007). Smaller streaks likely recorded incandescent rockfall or talus; such activity graded into larger block-and-ash flows.

On March 6, seismic vigor increased and clear daytime views revealed steaming and low-level ash emission that extended several hundred meters above the summit. Most of the steaming was on the north flank, and it appeared that the north lava flow that had effused during the end of the continuous phase was once again growing. No lava flow was visible in the northeast chute, although fresh, dark pyroclastic-flow deposits were visible, and a small pyroclastic flow was captured in motion at 1616 AKST by the Burr Point camera (table 1). Nighttime images showed that maximum incandescence occurred on March 6 and 7, when large swaths of the summit and upper north flank were glowing (fig. 18).

Seismicity quieted again for roughly 24 hours starting at 0600 AKST on March 7. Daytime views found no lava flow in the northeast chute on March 7 or 8. Starting at 0600 AKST on March 8, persistent, near-identical (drumbeat) earthquakes began to dominate the seismic signal (fig. 1; Power and Lalla, this volume). For 21 hours from 1730 AKST on March 8 to 1430 AKST on March 13, most on-island seismic stations received such strong signals that they were off the scale. By 1430 AKST on March 14, seismicity returned to pre-March 6 levels.

A lava flow was first observed within the northeast chute during an overflight on March 9. Observers also noted that pyroclastic-flow activity on March 9 was more prevalent to the northeast than to the north, suggesting active growth of the northeast lava flow during this time. That evening, nighttime cameras showed that the margin of the northeast lava flow was

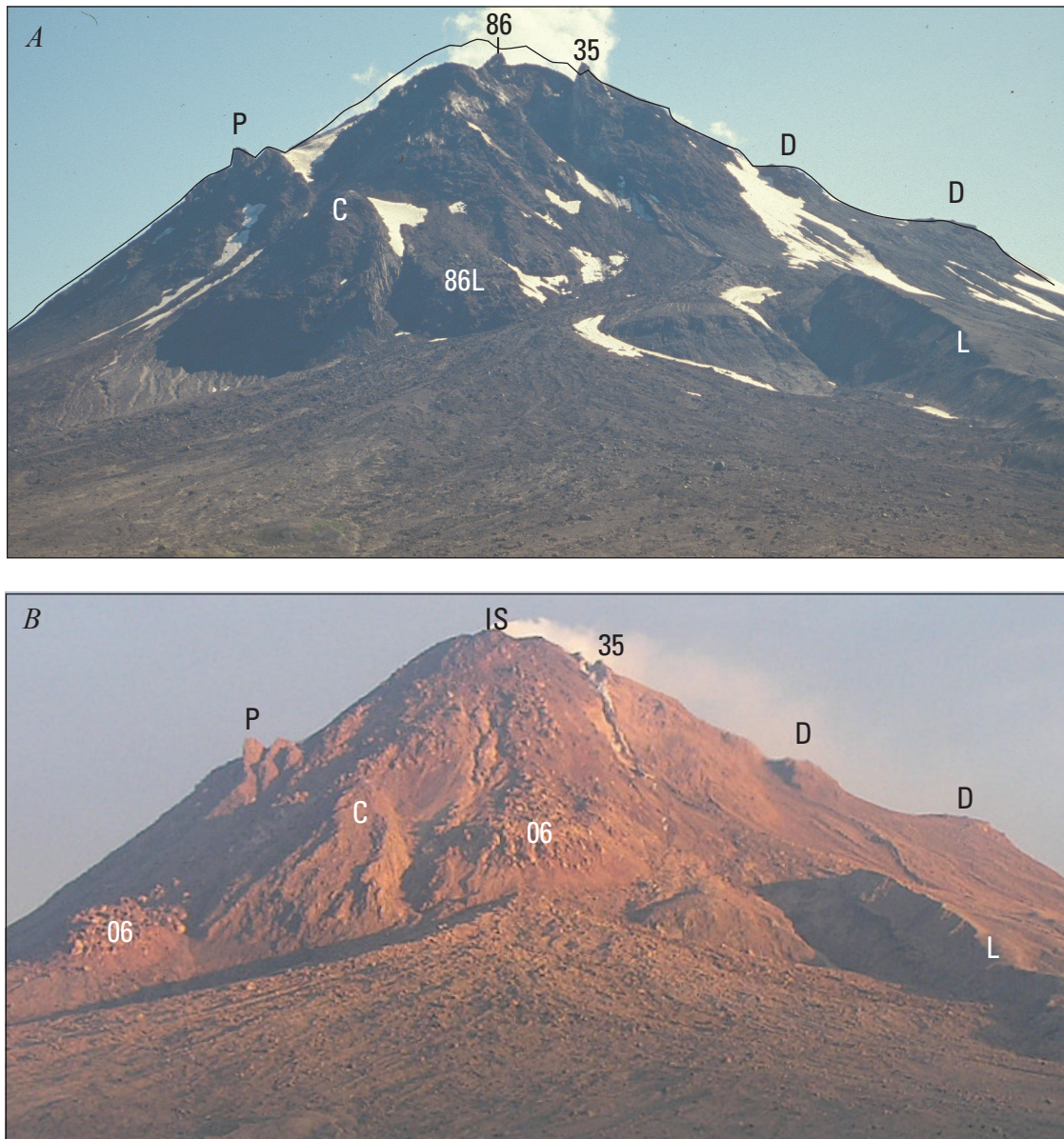


**Figure 19.** *A*, Augustine Volcano's edifice photographed from Burr Point to the north. Black line indicates edifice profile following the 2006 eruption. Photo by R.G. McGimsey, July 28, 1994. *B*, Augustine's edifice photographed from Burr Point time-lapse camera, July 24, 2006. P, Pinnacles (an old vent breccia; Swanson and Kienle, 1988); C, Cleaver; 86, 1986 lava spine; 35, 1935 dome remnant; D, prehistoric lava domes; 86L, lava flow from 1986 eruption; L, prehistoric north-flank lava flow; 06, lava flows from 2006 eruption; IS, incipient spine atop 2006 dome.

glowing. By March 14, areas of incandescence had moved down the slopes and marked the toes of the north and north-east lava flows (fig. 18).

Field crews flew to the island to acquire FLIR measurements twice during the effusive phase: on March 10 and March 15 (Wessels and others, this volume). Thermal images acquired on these dates delineate the new lava flows, whereas visual images were often partially obscured by steam, ash, and/or backlit conditions. On March 10, the new northeast lava flow was visible in thermal imagery and reached from

the top of the new summit dome to the base of the Cleaver, for a total length of roughly 1,000 m. The north lava flow had also advanced from its position at the end of the continuous phase—it measured about 900 m from the summit to the toe. By March 15, the northeast flow had lengthened to about 1,300 m, while the north lava flow had advanced only slightly, if at all. Both flows, however, appeared to have thickened considerably at their toes between March 10 and 15; the toe of the northeast flow was 80 m high, and that of the north lava flow was 85 m.

After March 15, the summit dome and the two lava flows underwent few or no morphological changes, indicating that effusion had largely ceased by that date. Incandescence also decreased and was limited to the west margin of the north lava flow (fig. 18).

The lava flows (unit Eflf; fig. 17; plate 1) from the 2006 eruption are typical of andesitic block lava flows and have prominent lateral levees, blocky surfaces, and steep flow fronts. The north flow is roughly 700 m long from the base of the new dome, as much as 340 m wide, and 85 m thick at the toe. The northeast lava flow extends 900 m from the base of the new dome, is as much as 250 m across, and is 80 m thick at the toe. They are the most voluminous of any lava flows from recent eruptions of Augustine Volcano. The 1986 eruption resulted in a steep blocky flow that appeared to issue from the base of the dome (Swanson and Kienle, 1988); it descended the north summit region to an altitude of approximately 580 m asl (fig. 19A). The 2006 north lava flow covered essentially all of that flow and is about as long, but it is about 200 m wider (fig. 19B). The 2006 northeast lava flow filled the northeast gully to an altitude of 500 m asl. The two lava flows are essentially continuous with the new summit dome, which covered the north halves of the flow lobes emplaced in January, and filled the north half of the summit crater from the 1935 dome remnant on the west to the informally named Pinnacles to the east (fig. 11; fig. 19B). The new dome now forms the volcano's summit, approximately 70 m higher than it was before 2006.

Lava effusion was accompanied by numerous rockfalls and small block-and-ash flows that were detected seismically (DeRoin and others, 2007), observed during overflights, and photographed by cameras. The block-and-ash flows formed prominent, dark deposits (unit Efba) that sit atop the upper reaches of the continuous-phase pyroclastic flows of the north and northeast fans (fig. 17; plate 1). Unit Efba flows also traveled down the east chute. These poorly sorted deposits consist of clasts of mostly dense andesite in a fine-grained matrix (Vallance and others, this volume).

## Post-Eruption Activity—Rock Avalanches and Lahars

While eruption of juvenile magma apparently ceased by March 16, secondary activity involving the remobilization of 2006 eruptive deposits continued through October 2006.

### Spring 2006 Rock Avalanches

On March 17 through 23, small, point-source incandescent areas were visible along the edges of the new lava flows. Rockfalls were recorded by seismic signals as often as a few times each day. Most signals recorded the downhill path of single, large boulders, as discovered in April when overflight observers saw a single boulder bounce down the west flank, marked the time, and found later that this activity correlated with a minute-long signal at nearby seismometer

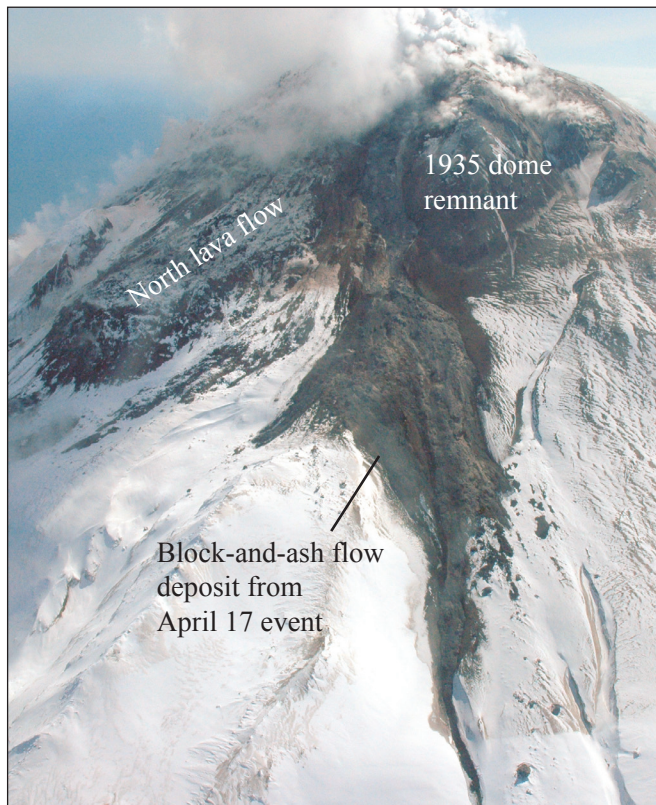


**Figure 20.** Photograph of Augustine Volcano's upper northwest flank, showing deposit from April 17 block-and-ash/rockfall event. Photo by R.G. McGimsey, April 19, 2006.



**Figure 21.** Photograph of Augustine Volcano's lower north flank, showing pink lahar deposits atop the 2006 Rocky Point pyroclastic-flow deposit. The lahars are thought to have occurred on October 1 and consist of remobilized fine-grained material from the 2006 eruptive deposits. Dark brown area at right of photo is pre-2006 surface. Field of view is approximately 500 m across. Photo by K.F. Bull, October 15, 2006.

AUW. Several longer, stronger seismic signals were found to correlate with larger rock-avalanche events.

The first rock-avalanche signals were detected on April 8. Between 1635 and 1708 AKDT, two bursts, 9 and 17 minutes long, were recorded seismically. Unfortunately, cloudy conditions at the time completely obscured the view from the Burr Point and Mound cameras. During a gas-monitoring flight on April 11, observers saw debris from the events (not present on an April 6 overflight) adjacent to the west margin of the north lava flow (table 1). The debris deposit extended almost as far downslope as the lava flow and had a total length of roughly 750 m. Large blocks—some steaming and some obviously cold—littered the area. A small lahar-like deposit extended downslope beyond the main debris field. Ash produced by this rock avalanche was carried by high winds across the northwest flank, leaving a radial, spoke-shaped deposit. Severely backlit conditions made it difficult to see the source area of the avalanche(s), but the axis of the deposit projected to a point below the summit dome. The deposit from this event was completely covered during subsequent activity, so it is not represented on the map (plate 1).

On April 17, a series of large flowage seismic signals, from 1656 to 1732 AKDT, were recorded by stations AUW, AUE, AUSE, and AUI. Elevated rockfall activity, recorded seismically, continued at a lesser rate until 0240 AKDT on the morning of April 18. Mound and Burr Point camera images from April 17 are obscured by clouds. During a gas-monitoring flight on April 19, observers saw a large amount of rock-avalanche debris on the volcano's northwest flank that had overrun the smaller debris field from April 8 (fig. 20). The main debris was not steaming, and they saw only a few hot blocks, mostly along the margin of the deposit. The distal end of the avalanche debris was incised and showed evidence of minor water flow. Backlit conditions once again prevented observations of the avalanche source area. The deposit was later partially covered by smaller rockfall events, but remnants of it are exposed and are shown on the deposit map as unit Pba (fig. 17; plate 1).

Rockfall activity increased again the night of May 25, leading to two particularly large flowage events on May 26 at 0106 and 0748 AKDT. The second event was the larger of the two and lasted approximately 5 minutes as recorded seismically. Unlike the previous avalanche events, the 0748 AKDT avalanche was photographed by both on-island cameras. Fortunately, it was also photographed by M. Byerly aboard a boat approximately 5 km northeast of Augustine Island (table 1). Images from the three sources show that the rock avalanche was accompanied by an ash cloud that likely rose to 1 to 2 km above the summit and drifted to the south. An initial small ash puff was recorded along the flank of the lava flow at 0738 AKDT, then a light-gray cloud moved downslope along the west side of the north lava flow, growing in height as it flowed almost to the end of the north-slope lava flow. By ~0800 AKDT, the flowage event had ended but the cloud had diffused, increased in diameter, and drifted around to the south and west side of the summit.

Observers on a June 2 overflight saw the deposits and located the source area of the May 26 events as the upper west side of the northwest lava flow, where a line of fumaroles down the chute marked the breakaway surface. The debris overtopped the upper portion of the north flank lava flow before bifurcating down either side; somewhat more debris was directed along the west side of the lava flow. The debris overlies deposits from previous slides.

## October 2006 Lahars

Several months after the cessation of eruptive activity, several small flowage events occurred, though these were different in nature than the spring rockfalls. On October 1, two pulses of seismicity were recorded from 0750 to 0915 (85 minutes) and 2116 to 2145 (29 minutes) AKDT. The signals were strongest on stations located on the east, north, and west flanks, and both were pulsatory with pulses from 2 to 10 minutes in duration (T. Petersen, written commun., 2006). These seismic signals had characteristics of surface clastic flows but persisted much longer than rockfall signals recorded previously.

On October 12 and 15, observers photographed new deposits on the lower north flank of the volcano (table 1). The new deposits were thin, braided, and obviously involved significant water in their emplacement (fig. 21). They were strikingly pinkish and light gray-colored, similar to pink ash-fall deposits associated with continuous-phase pyroclastic flow emplacement (Wallace and others, this volume). The largest of these October flow deposits was just south of the northeastern continuous-phase pyroclastic fan and reached the coastline. Others flowed atop Rocky Point and continuous-phase pyroclastic-flow deposits on the northwest flank, as well as on the west, south, and east sides. Where photographed on the north flank, new flows were most visible below a distinct break in slope at approximately 20 m asl. We believe that the observed lahar deposits correlate with the seismically detected events of October 1 and that they mostly involved remobilization of 2006 ash-fall deposits or matrix from continuous-phase pyroclastic-flow deposits. Deposits from these small-volume lahars are not shown on the 2006 geologic map (plate 1).

## Volume Calculations

### Methods

Using the geologic map, we have estimated the volumes of on-island erupted material from the eruptive phases of the 2006 Augustine Volcano activity (table 3; fig. 22). Most volumes were determined using the mapped areal extents of units and either estimating or measuring their thickness. Areas were measured from the time-slice maps (figs. 6, 8, 12, 17) to include buried deposits. The proximal, buried extents were either approximated or, where possible, mapped from imagery acquired during the eruption (for example, figs. 4

**Table 3.** Volume estimates for 2006 deposits.

[DRE, dense-rock equivalent; HSA, high-silica andesite; LSA, low-silica andesite]

Date (2006)	Deposit type (unit)	Deposit area (m <sup>2</sup> ) <sup>1</sup>	Deposit thickness (m)	Inflated eruptive volume (10 <sup>6</sup> m <sup>3</sup> )	Cumulative inflated erupted volume (10 <sup>6</sup> m <sup>3</sup> ) <sup>2</sup>	Erupted volume (DRE; 10 <sup>6</sup> m <sup>3</sup> )	Cumulative erupted volume (DRE; 10 <sup>6</sup> m <sup>3</sup> )	Cumulative erupted HSA (DRE; 10 <sup>6</sup> m <sup>3</sup> )	Cumulative erupted LSA (DRE; 10 <sup>6</sup> m <sup>3</sup> )	Duration (hr:min:sec)	Magma flux (m <sup>3</sup> /s)
Explosive phase											
January 11	Mixed avalanches (Exma)	980,000	n/a	n/a	n/a	n/a	n/a	n/a	n/a		
January 12	Early, ephemeral lava dome	n/a	n/a	n/a	n/a	n/a	n/a	n/a	n/a		
January 13–14	Events 3–8, flows (Expf, Expct, Exma, Exlh)	16,570,000	various	7.39	7.4 (1.9)	4.4	4.4	1.3	3.2		
January 13–14	Events 3–8, fall <sup>3</sup>	n/a	n/a	20.30	27.7	7.7	12.1	3.5	8.6	00:28:41	7,050
January 14–16	Lava dome (Exd1)	30,000	30	0.82	28.5 (2.0)	0.7	12.9	3.7	9.1	59:43:00	3
January 16–17	Continued growth of Exd1	70,000	30	2.06	30.5 (2.1)	1.8	14.7	4.3	10.4	19:58:00	25
January 17	Event 9, flow (Expf)	610,000	0.3	0.18	30.7 (2.1)	0.1	14.8	4.3	10.5	00:04:11	
January 17	Event 9, fall <sup>3</sup>	n/a	n/a	1.73	32.5	0.7	15.5	4.5	11.0	100:00:00	3,100
January 17–27	Lava dome (Exd2)	60,000	0.15	1.89	34.3 (2.2)	1.7	17.2	5.9	11.3	150:00:00	3
January 27–28	Events 10–13, flows (RPPf, Expc)	3,870,000	various	16.90	51.2 (3.7)	10.1	27.3	14.1	13.2		
January 27–28	Events 10–13, fall <sup>3</sup>	n/a	n/a	6.26	57.5	2.4	29.7	15.0	14.7	00:15:08	13,800
Continuous phase											
January 28–February 2	Flows (Cpf, Cpc, and Cpfw)	4,900,000	various	14.40	71.9 (5.2)	8.7	38.4	21.4	16.9	110:00:00	22
February 2–7	Lava flow (Efff)	220,000	50	10.80	82.7 (6.1)	9.6	47.9	22.5	25.4		
February 7–10	Continued lava growth (Efff)	30,000	50	1.50	84.2 (6.1)	1.3	49.3	22.6	26.6	192:00:00	16
Effusive phase											
February 10–March 3	Hiatus	0	0	0.00	84.2 (6.1)	0.0	49.3	22.6	26.6		
March 3–16	Lava flow and dome (Efff)	430,000	60	25.90	110.0 (8.9)	23.0	72.3	25.2	47.1		
March 6–16	Block and ash flows (Efba)	510,000	1	0.51	110.5 (8.9)	0.5	72.7	25.2	47.5	240:00:00	27

<sup>1</sup>Where referring to growing feature, like lava dome, deposit area refers to area of new growth only.<sup>2</sup>Uncertainty estimate given in parentheses.<sup>3</sup>Data from Wallace and others (this volume).

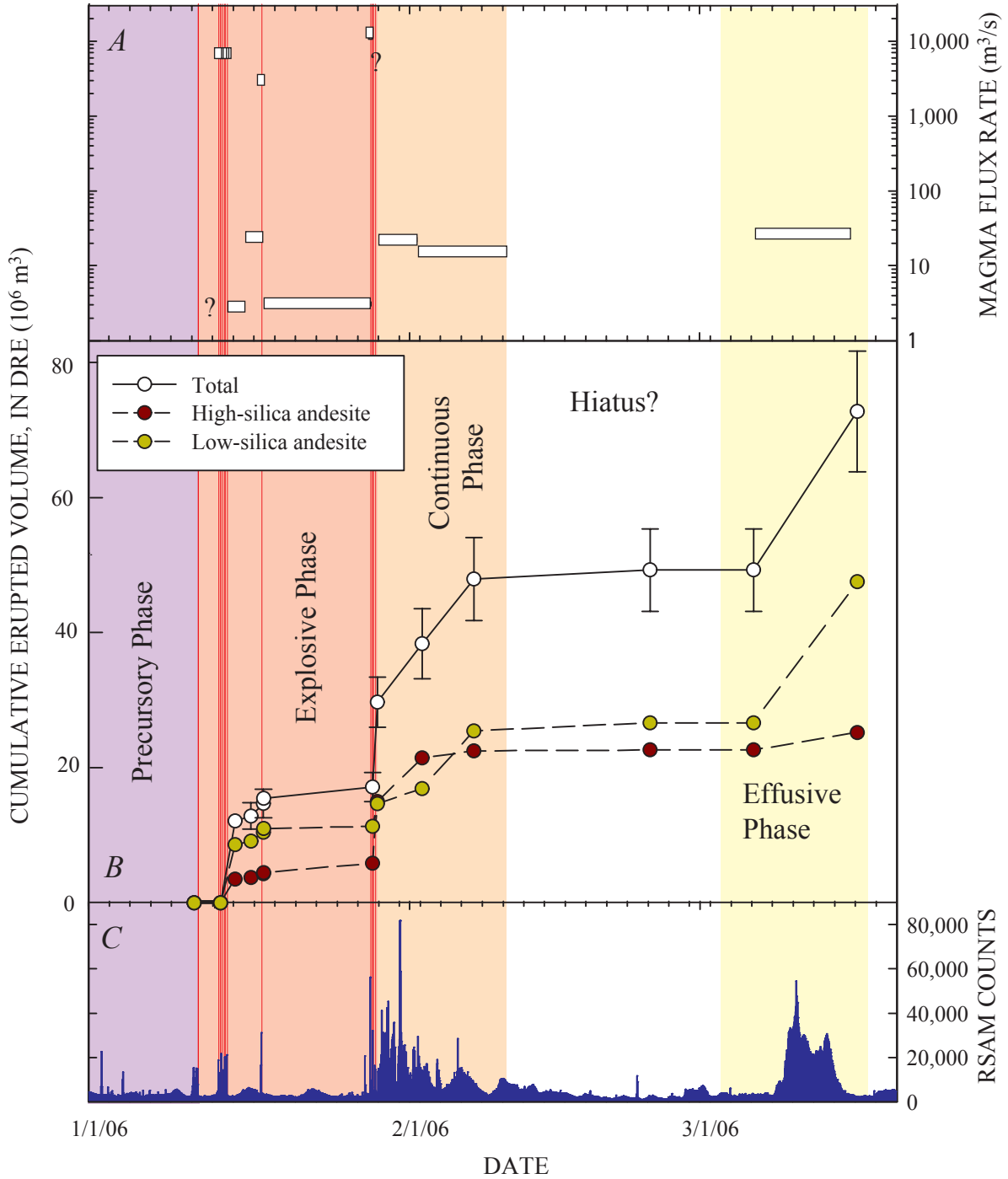


**Figure 22.** A, Magma flux rates (in dense-rock equivalent, or DRE) for intervals through the 2006 Augustine Volcano eruption. Flux rates plotted over red lines are for explosive events and have been calculated using the duration of the explosions; symbols have been enlarged for clarity. Flux rates that have been calculated for longer time periods are represented by bars. Note logarithmic scale. B, Cumulative erupted volume, in DRE, for the eruption. C, RSAM, or real-time seismic amplitude measurement, counts per day for Augustine station AU15. Explosive events 1–13 are shown as vertical red lines throughout A, B, and C.

and 5). Thicknesses of thinner pyroclastic-flow deposits were measured in the field (Vallance and others, this volume) and then averaged. The thicknesses of lava flows and domes were estimated or, where possible, measured from photographs and FLIR images (Wessels and others, this volume). For the continuous-phase and Rocky Point pyroclastic-flow deposits, volumes were calculated using digital terrain models (DTMs) generated by Aerometrics during the production of the orthophotos from January 4 and February 21, 2006. While these DTMs have unverified vertical accuracy, finding the difference of the two resulted in consistent volume gains over the mapped extents of the most voluminous pyroclastic flow deposits from late January and early February. Because field measurements of these deposits, many of which are several meters thick, were not possible in 2006, the values from the DTM differencing are presented here. Ash-fall volumes were calculated by Wallace and others (this volume) using the root-area method (Fierstein and Nathenson, 1992).

The main source of uncertainty in the calculations resides in the thickness measurements and/or estimates. These have propagated to the volumes and yield uncertainties of 25 to 50 percent. Inflated (erupted) volumes have been converted to dense-rock equivalent (DRE) using the following deposit/DRE ratios: 0.6 for fragmental flows, 0.9 for lava, and 0.4 for tephra-fall deposits.

Component analysis shows that each eruptive phase produced varying proportions of lithologic components (Vallance and others, this volume). Five dominant lithologies are low-silica andesite scoria; dense low-silica andesite; banded andesite; dense intermediate andesite; and high-silica andesite. We lump dense and scoriaceous low-silica andesite into a single compositional category and banded andesite and intermediate and high-silica andesite into another category to calculate volumetric estimates of two general compositional end members for each deposit (table 3). For lava flows, we assume they have the same proportions as block-and-ash flows shed from them; for domes, we assign composition based on the few of whole-rock analyses and surface appearance. Compositional ranges for the low- and high-silica andesite categories are 56 to 59 weight percent  $\text{SiO}_2$  and 59 to 63 weight percent  $\text{SiO}_2$ , respectively (Larsen and others, this volume).

## Results

The explosive phase produced about  $14.7 \times 10^6 \text{ m}^3$  as pyroclastic flows and  $10.8 \times 10^6 \text{ m}^3$  as tephra fall (these and all subsequent values given as dense rock equivalent, or DRE; table 3). The first explosive-phase lava dome, effused from January 14–17, had a volume of roughly  $2.5 \times 10^6 \text{ m}^3$ . The second dome, which effused between January 17 and 27, had a volume of roughly  $1.7 \times 10^6 \text{ m}^3$ . The total volume produced during the explosive phase was  $29.7 \times 10^6 \text{ m}^3$ . The largest single deposit of the eruption, the Rocky Point pyroclastic flow, erupted during event 10. During the explosive phase, low-silica and high-silica andesites were produced in nearly

equal amounts, though during the first half of this phase, low-silica andesite dominated (fig. 22).

Combining volume estimates with eruption intervals allows us to calculate magma flux rates, which show three brief periods of rapid magma release that coincide with explosive events, as well as much lower flux rates during times of dome growth and lava effusion. Using a cumulative duration of events 3–8 of 28 minutes, 41 seconds yields a magma flux of  $7,050 \text{ m}^3/\text{s}$  (table 3; fig. 22). Event 9 lasted for 4 minutes, 11 seconds and yields a flux of  $3,100 \text{ m}^3/\text{s}$  (table 3). During events 10–13 on January 27 and 28, which cumulatively lasted 15 minutes, the calculated flux rate is roughly  $14,000 \text{ m}^3/\text{s}$ ; this high rate corresponds with the eruption of the voluminous Rocky Point pyroclastic-flow deposit during event 10. The flux rates for the dome-building interval of January 14–17 and January 17–27 are much lower:  $3\text{--}25 \text{ m}^3/\text{s}$  and  $3 \text{ m}^3/\text{s}$ , respectively. If, however, explosive-phase lava dome 2 began growing later than January 17, the rate at which it effused could be much higher.

During the early continuous phase (January 28 through February 2), the volcano erupted  $8.7 \times 10^6 \text{ m}^3$  of magma in the form of pyroclastic-flow deposits. The volume of fallout tephra produced during this time is uncertain but was likely volumetrically minor (Wallace and others, this volume). As the vigor of the continuous phase waned,  $9.6 \times 10^6 \text{ m}^3$  of lava effused. Assuming continuous eruption during this period, the flux rate during the early continuous phase was  $22 \text{ m}^3/\text{s}$  and dropped to  $16 \text{ m}^3/\text{s}$  during its less vigorous second half. As shown by component studies (Vallance and others, this volume), the high-silica-andesite compositional end member dominated the first half of this phase, producing about three quarters, or  $6.4 \times 10^6 \text{ m}^3$ , of the magma that fed the pyroclastic flows. The compositions of the lava flow and dome that effused during the second half of the continuous phase are less well known but, on the basis of appearance, are interpreted to be similar to that of the final lava flows—rich in low-silica andesite.

After an apparent hiatus from roughly February 10 through March 3, when no new magma was erupted, the effusive phase produced approximately  $23.5 \times 10^6 \text{ m}^3$  of lava and block-and-ash flows. Ash-fallout volumes were again likely minor during this interval (Wallace and others, this volume). This phase of the eruption was dominated by the low-silica-andesite end member, which accounted for roughly  $20 \times 10^6 \text{ m}^3$  of lava effused. The magma flux rate during the effusive phase was approximately  $27 \text{ m}^3/\text{s}$ , assuming constant effusion over this interval.

## Eruptive Mechanisms During The 2006 Eruption

The 2006 and other recent eruptions of Augustine Volcano share similarities with other intermediate-composition, dome-building volcanoes worldwide. In general, however,

Augustine seems to have briefer, more intense eruptive cycles compared to other dome-forming volcanoes, such as Mount St. Helens in Washington, Unzen volcano in Japan, Soufriere Hills volcano on Montserrat, or Santiaguito volcano in Guatemala, where eruption cycles typically last years (Rose, 1987; Swanson and Holcomb, 1990; Nakada and others, 1999; Kokelaar, 2002). We discuss the eruptive mechanisms responsible for the varying styles of the three eruptive phases of Augustine Volcano in 2006 and the corresponding activity in previous eruptions.

## The Explosive Phase—Cyclic Vulcanian Explosions

The explosive phase of the 2006 eruption consisted of a series of discrete explosions, each minutes long, separated by periods of hours to days. Events 1 and 2 on January 11 produced cold mixed avalanches of snow, rock, and ice and fine-grained tephra-fall deposits that appear to contain little or no juvenile material (Wallace and others, this volume). We conclude that little or no magma had reached the shallow edifice and that the explosions were driven by ascending gases that had accumulated beneath the summit.

In contrast, events 3–13 produced ash-rich plumes, pyroclastic flows, and surges and resulting lahars and mixed avalanches that traveled far down all slopes of the volcano. Thus, the main magmatic eruption commenced on January 13. Pyroclastic-flow deposits from these events were not topographically confined and were likely formed during partial collapse of an eruptive column.

We were not able to calculate volumes for each individual event, but for those that we could, the volume varied dramatically. During event 9, the total volume erupted as both fall and flow deposits was  $\sim 0.8 \times 10^6 \text{ m}^3$ , whereas the volume of flow deposits from event 10 was  $10 \times 10^6 \text{ m}^3$  (both in DRE; table 3). For events 3 through 8, the total erupted volume was  $12.1 \times 10^6 \text{ m}^3$ , which yields an average volume per event of roughly  $2 \times 10^6 \text{ m}^3$ . For these events we calculate magma flux rates of 103 to  $104 \text{ m}^3/\text{s}$ . Because explosive events 11 through 13 were closely followed by the beginning of the continuous phase, volumes of deposits from these explosions are less well known.

Many of these characteristics are shared by other vulcanian explosions during previous eruptions of Augustine Volcano (Kienle and Shaw, 1979) and other andesitic volcanoes worldwide, including Soufriere Hills, Montserrat (Druitt and others, 2002); Mount Ngauruhoe, New Zealand (Nairn and Self, 1978); Lascar Volcano, Chile (Matthews and others, 1997); Mount Pinatubo, Philippines (Hoblitt and others, 1996); and Galeras Volcano, Columbia (Stix and others, 1997). Vulcanian explosions are attributed to two main mechanisms: either the interaction of magma with external water, or, as in the cases cited here, the sudden release of pressurized magma beneath a cooled or degassed lava cap (Self and others, 1979; Sparks, 1997; Stix and others, 1997; Morrissey and Mastin, 2000).

A consistent model that accounts for vulcanian explosions at other andesitic, dome-building volcanoes (Druitt and others, 2002) involves a shallow conduit filled with pressurized, vesicular magma, capped by degassed magma in the form of a lava dome or plug. As magma rises into the conduit from below and/or shallow crystallization causes vapor exsolution, increased conduit overpressure exceeds the strength of the cap (Sparks, 1997). At this point the cap is destroyed and a fragmentation wave descends into the conduit creating rapidly escalating conduit escape velocities and the formation of an ash-rich plume. The onset of the explosion is thought to be accompanied by a shock wave (Morrissey and Mastin, 2000). This phase is highly unstable and lasts seconds to minutes. Once the fragmentation wave reaches a level in the conduit where pressure is not great enough to drive fragmentation, the explosion greatly lessens in intensity or stops. Then the conduit refills, eventually leading to another degassed solid cap at the top, and the cycle repeats.

Only about half of the explosive events during the 2006 Augustine Volcano explosive phase had the impulsive acoustic waveforms that would result from the initial shock wave typical of vulcanian blasts (Petersen and others, 2006). The acoustic signal from event 1 was large and impulsive, consistent with this event acting as a vent clearing. The next impulsive event was event 5, which produced significant flows down the north flank. Events 8 through 12 were either impulsive or both emergent plus impulsive (Petersen and others, 2006). One explanation for the mix in waveforms is that some recorded partial failures of lava domes or plugs in addition to impulsive gas release.

By estimating the conduit dimension and erupted volume of each event, we can estimate the depth to which each explosion might have evacuated the conduit. We estimate the vent for the 2006 eruption to be roughly 30 by 45 m, elongate in the north-northwest–south-southeast direction, based on the location of an incipient spine atop the final dome (figs. 17, 19B); we assume the conduit will retain these dimensions. Events 3–8 each discharged approximately  $2 \times 10^6 \text{ m}^3$  of magma, which yields an average evacuation of the conduit to 1.9 km below the summit. If we have underestimated the dimension of the conduit and instead use a diameter of 50 m (similar to that of the 1986 spine), we calculate an average evacuation depth to 1 km. Such depths are consistent with those calculated for vulcanian explosions that occurred in 1997 at Soufriere Hills volcano, Montserrat (Druitt and others, 2002).

Event 10 was the largest of the explosive blasts, producing roughly  $12.5 \times 10^6 \text{ m}^3$  (DRE) of magma. Some of the material in the event 10 flow deposits is likely the destroyed portion of the explosive-phase dome 2. This dome had a volume of  $1.7 \times 10^6 \text{ m}^3$  prior to event 10, and slightly less than half was destroyed during this event. Using a conservative estimate of  $0.8 \times 10^6 \text{ m}^3$  as contributing to the volume of the event 10 flow deposits, juvenile magma erupted during this event would have been roughly  $11.7 \times 10^6 \text{ m}^3$  (DRE). A distinct compositional shift, from predominantly low-silica andesite to predominantly high-silica andesite, occurred

during event 10 between emplacement of the explosive-phase pyroclastic-current and Rocky Point pyroclastic-flow deposits (Vallance and others, this volume). Assuming that all of the juvenile magma was evacuated from a conduit with the dimensions above would result in a conduit length of over 11 km! Petrologic and geodetic evidence suggest, however, that the magma storage region that held the erupted high-silica andesite is located at a depth of roughly 5 km below the summit (Larsen and others, this volume; Cervelli and others, this volume), consistent with post-eruption earthquake hypocenters located at this depth (Power and Lalla, this volume). If this is accurate, event 10 likely evacuated the entire conduit and partially evacuated the magma storage region, whether the latter was a chamber, dike, sill, or crystal-mush zone. This is particularly intriguing given the compositional shift that occurred during this event and suggests that the low-silica andesite erupted during the first half of event 10 came from the conduit and that the high-silica andesite erupted during the second half of the event came predominantly from the magma storage region. This also suggests that this event may have cleared the way for the subsequent eruption of large volumes of high-silica andesite during the continuous phase.

An additional constraint on magma movement and withdrawal prior to and during the vulcanian blasts comes from GPS data that show a shallow inflationary source at sea level that was present from June through November of 2005 (Cervelli and others, 2006). Cervelli and others model this as the result of a point source near sea level that pressurized at a rate corresponding to  $4 \times 10^5 \text{ m}^3/\text{yr}$ , or a volume change of  $2 \times 10^5 \text{ m}^3$  (Cervelli and others, 2006). This volume is an order of magnitude lower than material erupted during any one of the explosions, thus we suggest that this sea-level inflationary signal was caused by pressurization by magmatic gas, not magma. This pressurization may have been facilitated by the presence of the relatively impermeable zeolitized Naknek Formation near sea level beneath Augustine Volcano (Detterman and Reed, 1980). On November 17, following the 6-month-long signal, a much stronger inflationary signal began at the summit stations and lasted until January 12. The stronger signal has been modeled as the ascent of a north-south-trending dike from near sea level to the summit (Cervelli and others, 2006). Upward earthquake migration was detected in this depth range during the same time interval (DeShon and others, this volume; Power and Lalla, this volume). We suggest that this dike possessed a gas-filled tip that preceded new magma to the surface, culminating in the gas-rich but juvenile-magma-poor January 11 explosions. Magma then reached the surface on January 12 in the form of a lava dome; growing overpressure in the conduit caused vulcanian magmatic blasts to begin on January 13.

## The Continuous Phase—Dome Growth and Collapse

The onset of the continuous phase heralded a distinct shift in eruptive style from the explosive phase. This phase

was mainly characterized by pyroclastic-flow emplacement that tapered to lava effusion, but activity began the afternoon of January 28 with a two-hour-long period of volcanic tremor and accompanying ash emission. It was not until 2200 AKST the night of January 28 that the first flowage-type seismic signals were detected. Later observations, and discovery of a seismic station destroyed during this interval, revealed that each signal represented a pyroclastic flow of varying size. This activity continued until February 3, when slower effusion apparently led to the formation of a small lava flow.

By evaluating the volumes of erupted pyroclastic flows from this period, we can evaluate whether pyroclastic flows formed primarily as the result of a collapsing, preexisting dome or whether the dome was actively growing during this interval. The first half of the continuous phase produced more than  $14 \times 10^6 \text{ m}^3$  of erupted material (not DRE). A circular dome of this volume, if 40 m tall, would have a radius of  $\sim 340 \text{ m}$ , which would more than cover the entire summit area. This indicates that pyroclastic flows during this period were not just the result of collapse of an existing lava dome but were instead occurring during active effusion and rapid collapse of a growing dome. Satellite imagery from the middle of this period shows that a roughly circular dome was present at the summit and that flows were initiating from its margins.

Similar activity has been recorded at other dome-forming volcanoes, notably Mount Merapi in Indonesia, Soufriere Hills in Montserrat, and Unzen in Japan. Often, periods of block-and-ash flow activity of this intensity are shorter, however, and thought to be due to collapse of a static dome. For example, on November 22, 1994, roughly  $3 \times 10^6 \text{ m}^3$  of block-and-ash flows formed over a 7-hour interval at Merapi when a portion of the summit lava dome collapsed (Abdurachman and others, 2000).

The continuous-phase activity is consistent with relatively high initial magma-flux rates that resulted in rapid effusion and almost continual collapse of a growing lava dome. The composition of this dome was predominantly high-silica andesite, unlike the low-silica-andesite-dominated explosive phase. As the dome grew, its margins became unstable and collapsed, forming classic, Merapi-style block-and-ash flows. Most of these traveled to the north and northeast of the summit, forming composite pyroclastic fans much like those formed during the 1976 and 1986 eruptions of the volcano. At least two larger pyroclastic flows, however, were emplaced early in the continuous phase, including the windy pyroclastic flow that erupted on January 30. These flows occurred when larger portions of the lava dome collapsed, or they reflect fluctuations in magma flux.

As magma flux at the conduit waned, lava that reached the surface remained intact to form a new dome and a short steep lava flow to the north. We did not sample the lava flow at this stage, but images from February show that debris from this lava tongue is much darker than underlying flowage deposits from earlier in the continuous phase, suggesting that the composition had perhaps transitioned to the low-silica andesite that erupted later in the effusive phase.

## The Effusive Phase—Rapid Effusion of Lava and Block-and-Ash Flows

The flux rate calculated during the effusive-phase rate of  $\sim 27 \text{ m}^3/\text{s}$  is quite high compared to other rates of lava effusion measured elsewhere. During periods of exogenous dome growth between 1980 and 1986, extrusion rates at Mount St. Helens varied from 1.4 to  $40.3 \text{ m}^3/\text{s}$  (Anderson and Fink, 1990), similar to or higher than the rates at Augustine Volcano. However, at Santiaguito in Guatemala, dome growth varied between periods of slow ( $0.16 \text{ m}^3/\text{s}$ ) and relatively fast ( $0.6\text{--}1.9 \text{ m}^3/\text{s}$ ) extrusion (Rose, 1987). At Mount Merapi in Indonesia, from 1984–1995, lava-dome effusion rates varied from 0.05 to  $0.32 \text{ m}^3/\text{s}$ , with an average long-term rate of  $0.039 \text{ m}^3/\text{s}$  (Siswawidjono and others, 1995). Thus, while effusion occurred over a short time period in March of 2006, the resulting volume was equivalent to that seen for domes/flows elsewhere erupted over much longer periods.

The block-and-ash flows during the effusive phase are much smaller in volume than flows from the continuous phase. They are similar to other classic deposits of this type seen at Unzen Volcano in Japan and elsewhere. At Unzen, Ui and others (1999) describe block-and-ash flows that occur when lava is actively flowing downslope, and the tensile strength of the deforming lava is exceeded by the pore pressure in the lava and the downslope tensional force. This causes a local explosion, often around a growing crack, and fragmentation is triggered at the lobe front—a likely explanation for the effusive-phase pyroclastic flows at Augustine Volcano.

The rock-avalanche events that occurred at Augustine Volcano in April and May, well after effusion had ceased, still resulted in observed ash clouds and block-and-ash-flow-type deposits. We suggest that these events resemble rockfall-induced block-and-ash flows that also occurred at Unzen (Ui and others, 1999). The steep slopes near Augustine's summit led to rock falls off the western edge of the still-hot north lava flow. As blocks of hot lava that retained high pore pressures hit the ground, they fragmented upon impact causing small block-and-ash flows. The rockfalls off the north lava flow occurred repeatedly from the same location, exposing fresh parts of the flow interior that had not been fully degassed. This may explain why each block-and-ash flow was somewhat bigger than the last.

## Acknowledgments

We thank the entire staff of the Alaska Volcano Observatory (AVO) for their efforts during the 2006 Augustine eruption—without the detailed observations made by many, this paper would not have been possible. In particular, we are grateful for conversations with Peter Cervelli, Pavel Izbekov, Steve McNutt, Tina Neal, Chris Nye, John Power, Stephanie Prejean, and Kristi Wallace that helped us to refine our chronology of events and our ideas about eruptive mechanisms. Comments by Wes Hildreth, John Power,

and in particular Tom Sisson improved the manuscript. We also thank the skilled helicopter and fixed-wing pilots who took us to the volcano despite often-challenging conditions. A special thanks to Cheryl Cameron and Seth Snedigar, who have made the AVO image database and other web-based tools that are so useful.

## References Cited

- Abdurachman, E.K., Bourdier, J.-L., and Voight, B., 2000, Nuées ardentes of 22 November 1994 at Merapi volcano, Java, Indonesia: *Journal of Volcanology and Geothermal Research*, v. 100, p. 345–361.
- Anderson, S., and Fink, J.H., 1990, The development and distribution of lava textures at the Mount St. Helens dome, *in* Fink, J.H., ed., *Lava flows and domes; emplacement mechanisms and hazard implications*: Berlin, Springer-Verlag, International Association of Volcanology and Chemistry of the Earth's Interior, p. 25–46.
- Bailey, J.E., Dean, K.G., Dehn, J., and Webley, P.W., 2010, Integrated satellite observations of the 2006 eruption of Augustine Volcano, *in* Power, J.A., Coombs, M.L., and Freymueller, J.T., eds., *The 2006 eruption of Augustine Volcano, Alaska*: U.S. Geological Survey Professional Paper 1769 (this volume).
- Begét, J.E., and Kienle, J., 1992, Cyclic formation of debris avalanches at Mount St. Augustine volcano: *Nature*, v. 356, no. 6371, p. 701–704.
- Cervelli, P.F., Fournier, T., Freymueller, J.T., and Power, J.A., 2006, Ground deformation associated with the precursory unrest and early phases of the January 2006 eruption of Augustine Volcano, Alaska: *Geophysical Research Letters*, v. 33, L18304, doi:10.1027/2006GL027219.
- Cervelli, P.F., Fournier, T.J., Freymueller, J.T., Power, J.A., Lisowski, M., and Pauk, B.A., 2010, Geodetic constraints on magma movement and withdrawal during the 2006 eruption of Augustine Volcano, *in* Power, J.A., Coombs, M.L., and Freymueller, J.T., eds., *The 2006 eruption of Augustine Volcano, Alaska*: U.S. Geological Survey Professional Paper 1769 (this volume).
- DeRoin, N., McNutt, S.R., Reyes, C., and Sentman, D.D., 2007, Rockfalls at Augustine Volcano, Alaska; 2003–2006: *Eos Transactions of the American Geophysical Union*, v. 88, S43–1038.
- DeShon, H.R., Thurber, C.H., and Power, J.A., 2010, Earthquake waveform similarity and evolution at Augustine Volcano from 1993 to 2006, *in* Power, J.A., Coombs, M.L., and Freymueller, J.T., eds., *The 2006 eruption of Augustine Volcano, Alaska*: U.S. Geological Survey Professional Paper 1769 (this volume).

- Detterman, R.L., and Reed, B.L., 1980, Stratigraphy, structure, and economic geology of the Iliamna quadrangle, Alaska: U.S. Geological Survey Bulletin 1368-B, 86 p, 1 sheet.
- Druitt, T.H., Young, S.R., Baptie, B., Bonadonna, C., Calder, E.S., Clarke, A.B., Cole, P.D., Harford, C.L., Herd, R.A., Luckett, R., Ryan, G., and Voight, B., 2002, Episodes of cyclic Vulcanian explosive activity with fountain collapse at Soufriere Hills Volcano, Montserrat, *in* Druitt, T.H., and Kokelaar, B.P., eds., *The Eruption of Soufriere Hills Volcano, Montserrat, from 1995 to 1999*: London, The Geological Society, p. 281–306.
- Dzurisin, D.J., Vallance, J.W., Gerlach, T.M., Moran, S.C., and Malone, S.D., 2005, Mount St. Helens reawakens: Eos (American Geophysical Union Transactions), v. 86, no. 3, p. 25, 29.
- Fierstein, J., and Nathenson, M., 1992, Another look at the calculation of fallout tephra volumes: *Bulletin of Volcanology*, v. 54, p. 156–167.
- Hoblitt, R.P., Wolfe, E.W., Scott, W.E., Couchman, M.R., Pallister, J.S., and Javier, D., 1996, The pre-climactic eruptions of Mount Pinatubo, June 1991, *in* Newhall, C.G., and Punongbayan, R.S., eds., *Fire and Mud; eruptions and Lahars of Mount Pinatubo, Philippines*: Seattle, University of Washington Press, p. 457–511.
- Johnston, D.A., 1978, Volatiles, magma mixing, and the mechanism of eruption at Augustine Volcano, Alaska: University of Washington Ph.D. dissertation, 187 p.
- Johnston, D.A., 1979, Onset of volcanism at Augustine Volcano, lower Cook Inlet, *in* Johnson, K.M. and Williams, J.R., Jr., eds., *The United States Geological Survey in Alaska; accomplishments during 1978*: U.S. Geological Survey Circular 0804-B, p. B78–B80.
- Kamata, H., Johnston, D.A., and Waitt, R.B., 1991, Stratigraphy, chronology, and character of the 1976 pyroclastic eruption of Augustine Volcano, Alaska: *Bulletin of Volcanology*, v. 53, p. 407–409.
- Kienle, J., and Shaw, G.E., 1979, Plume dynamics, thermal energy, and long-distance transport of vulcanian eruption clouds from Augustine Volcano, Alaska: *Journal of Volcanology and Geothermal Research*, v. 6, p. 139–164.
- Kokelaar, B.P., 2002, Setting, chronology, and consequences of the eruption of Soufriere Hills Volcano, Montserrat (1995–1999), *in* Druitt, T.H., and Kokelaar, B.P., eds., *The Eruption of Soufriere Hills Volcano, Montserrat, from 1995–1999*: London, The Geological Society, p. 1–44.
- Larsen, J.F., Nye, C.J., Coombs, M.L., Tilman, M., Izbekov, P., and Cameron, C., 2010, Petrology and geochemistry of the 2006 eruption of Augustine Volcano, *in* Power, J.A., Coombs, M.L., and Freymueller, J.T., eds., *The 2006 eruption of Augustine Volcano, Alaska*: U.S. Geological Survey Professional Paper 1769 (this volume).
- Matthews, S.J., Gardeweg, M.C., and Sparks, R.S.J., 1997, The 1984–1996 cyclic activity of Lascar Volcano, northern Chile; cycles of dome growth, dome subsidence, degassing and explosive eruptions: *Bulletin of Volcanology*, v. 59, p. 72–82.
- McNutt, S.R., Tytgat, G., Estes, S.A., and Stihler, S.D., 2010, A parametric study of the January 2006 explosive eruptions of Augustine Volcano, using seismic, infrasonic, and lightning data *in* Power, J.A., Coombs, M.L., and Freymueller, J.T., eds., *The 2006 eruption of Augustine Volcano, Alaska*: U.S. Geological Survey Professional Paper 1769 (this volume).
- Morrissey, M.M., and Mastin, L.G., 2000, Vulcanian eruptions, *in* Sigurdsson, H., Houghton, B.F., McNutt, S.R., Rymer, H., and Stix, J., eds., *Encyclopedia of volcanoes*: San Diego, Academic Press, p. 463–475.
- Nairn, I.A., and Self, S., 1978, Explosive avalanches and pyroclastic flows from Ngauruhoe 1975: *Journal of Volcanology and Geothermal Research*, v. 3, p. 39–60.
- Nakada, S., Shimizu, H., and Ohta, K., 1999, Overview of the 1990–1995 eruption at Unzen Volcano: *Journal of Volcanology and Geothermal Research*, v. 89, p. 1–22.
- Neal, C.A., Murray, T.L., Power, J.A., Adleman, J.N., Whitmore, P.M., and Osiensky, J.M., 2010, Hazard information management, interagency coordination and impacts of the 2005–2006 eruption of Augustine Volcano, *in* Power, J.A., Coombs, M.L., and Freymueller, J.T., eds., *The 2006 eruption of Augustine Volcano, Alaska*: U.S. Geological Survey Professional Paper 1769 (this volume).
- Paskievitch, J., Read, C., and Parker, T., 2010, Remote tele-metered and time-lapse cameras at Augustine Volcano, *in* Power, J.A., Coombs, M.L., and Freymueller, J.T., eds., *The 2006 eruption of Augustine Volcano, Alaska*: U.S. Geological Survey Professional Paper 1769 (this volume).
- Pauk, B.A., Jackson, M., Feaux, K., Mencin, D., and Bohnenstiehl, K., 2010, The Plate Boundary Observatory permanent global positioning system network on Augustine Volcano before and after the 2006 eruption, *in* Power, J.A., Coombs, M.L., and Freymueller, J.T., eds., *The 2006 eruption of Augustine Volcano, Alaska*: U.S. Geological Survey Professional Paper 1769 (this volume).
- Petersen, T., De Angelis, S., Tytgat, G., and McNutt, S.R., 2006, Local infrasound observations of large ash explosions at Augustine Volcano, Alaska, during January 11–28, 2006: *Geophysical Research Letters*, v. 33, L12303, doi:10.1029/2006GL026491.
- Power, J., 1988, Seismicity associated with the 1986 eruption of Augustine Volcano, Alaska: Fairbanks, University of Alaska, unpub. M.S. thesis, 142 p.

- Power, J.A., and Lalla, D.J., 2010, Seismic observations of Augustine Volcano, 1970–2007, *in* Power, J.A., Coombs, M.L., and Freymueller, J.T., eds., *The 2006 eruption of Augustine Volcano, Alaska: U.S. Geological Survey Professional Paper 1769* (this volume).
- Power, J.A., Nye, C.J., Coombs, M.L., Wessels, R.L., Cervelli, P.F., Dehn, J., Wallace, K.L., Freymueller, J.T., and Doukas, M.P., 2006, The reawakening of Alaska's Augustine Volcano: *Eos* (American Geophysical Union Transactions), v. 87, no. 37, p. 373, 377.
- Rose, W.I., 1987, Volcanic activity at Santiaguito volcano, 1976–1984, *in* Fink, J.H., ed., *The emplacement of silicic domes and lava flows: Boulder, Colo., The Geological Society of America*, p. 17–28.
- Schneider, D.J., Scott, C., Wood J., and Hall T., 2006, NEXRAD weather radar observations of the 2006 Augustine volcanic eruption clouds: *Eos* (American Geophysical Union Transactions), v. 87, Abstract V51C–1686.
- Self, S., Wilson, L., and Nairn, I.A., 1979, Vulcanian eruption mechanisms: *Nature*, v. 277, p. 440–443.
- Sentman, D.D., McNutt, S.R., Stenbaek-Nielsen, H.C., Tytgat, G., and DeRoin, N., 2010, Imaging observations of thermal emissions from Augustine Volcano using a small astronomical camera, *in* Power, J.A., Coombs, M.L., and Freymueller, J.T., eds., *The 2006 eruption of Augustine Volcano, Alaska: U.S. Geological Survey Professional Paper 1769* (this volume).
- Siswowidjoyo, S., Suryo, I., and Yokoyama, I., 1995, Magma eruption rates of Merapi volcano, central Java, Indonesia during one century (1890–1992): *Bulletin of Volcanology*, v. 57, p. 111–116.
- Sparks, R.S.J., 1997, Causes and consequences of pressurisation in lava dome eruptions: *Earth and Planetary Science Letters*, v. 150, p. 177–189.
- Stith, J.L., Hobbs, P.V., and Radke, L.F., 1977, Observations of a nuee ardente from the St. Augustine Volcano: *Geophysical Research Letters*, v. 4, p. 259–262.
- Stix, J., Torres, R.C., Narvaez, M.L., Cortes, G.P., Raigosa, J.A., Gomez, D.M., and Castonguay, R., 1997, A model of Vulcanian eruptions at Galeras Volcano, Columbia: *Journal of Volcanology and Geothermal Research*, v. 77, p. 285–304.
- Swanson, D.A., and Holcomb, R.T., 1990, Regularities in growth of the Mount St. Helens dacite dome, 1980–1986, *in* Fink, J.H., ed., *Lava flows and domes; emplacement mechanisms and hazard implications: Berlin, Springer-Verlag, International Association of Volcanology and Chemistry of the Earth's Interior*, p. 3–24.
- Swanson, S.E., and Kienle, J., 1988, The 1986 eruption of Mount St. Augustine; field test of a hazard evaluation: *Journal of Geophysical Research*, v. 93, p. 4500–4520.
- Thomas, R.J., McNutt, S.R., Krehbiel, P.R., Rison, W., Aulich, G., Edens, H.E., Tytgat, G., and Clark, E., 2010, Lightning and electrical activity during the 2006 eruption of Augustine Volcano, *in* Power, J.A., Coombs, M.L., and Freymueller, J.T., eds., *The 2006 eruption of Augustine Volcano, Alaska: U.S. Geological Survey Professional Paper 1769* (this volume).
- Ui, T., Matsuwo, N., Sumita, M., and Fujinawa, A., 1999, Generation of block and ash flows during the 1990–1995 eruption of Unzen Volcano, Japan: *Journal of Volcanology and Geothermal Research*, v. 89, p. 123–138.
- Vallance, J.W., Bull, K.F., and Coombs, M.L., 2010, Pyroclastic flows, lahars, and mixed avalanches generated during the 2006 eruption of Augustine Volcano, *in* Power, J.A., Coombs, M.L., and Freymueller, J.T., eds., *The 2006 eruption of Augustine Volcano, Alaska: U.S. Geological Survey Professional Paper 1769* (this volume).
- Watt, R.B., and Begét, J.E., 2009, Volcanic processes and geology of Augustine Volcano, Alaska: U.S. Geological Survey Professional Paper 1762, 78 p., 2 map plates [<http://pubs.usgs.gov/pp/1762/>].
- Wallace, K.L., Neal, C.A., and McGimsey, R.G., 2010, Timing, distribution, and character of tephra fall from the 2005–2006 eruption of Augustine Volcano, *in* Power, J.A., Coombs, M.L., and Freymueller, J.T., eds., *The 2006 eruption of Augustine Volcano, Alaska: U.S. Geological Survey Professional Paper 1769* (this volume).
- Wessels, R.L., Coombs, M.L., Schneider, D.J., Dehn, J., and Ramsey, M.S., 2010, High-resolution satellite and airborne thermal infrared imaging of the 2006 eruption of Augustine Volcano, *in* Power, J.A., Coombs, M.L., and Freymueller, J.T., eds., *The 2006 eruption of Augustine Volcano, Alaska: U.S. Geological Survey Professional Paper 1769* (this volume).
- Yount, E.M., Miller, T.P., and Gamble, B.M., 1987, The 1986 eruptions of Augustine Volcano, Alaska, hazards and effects, *in* Hamilton, T.D., and Galloway, J.P., eds., *The United States Geological Survey in Alaska; accomplishments during 1986: U.S. Geological Survey Circular 0998*, p. 4–13.